



HAL
open science

Effect of surface curing temperature on depth-specific physical properties of Poly(urethane-isocyanurate) foam panels in relation with local chemical composition and morphology

Joël Reignier, Françoise Méchin, Alexandru Sarbu

► **To cite this version:**

Joël Reignier, Françoise Méchin, Alexandru Sarbu. Effect of surface curing temperature on depth-specific physical properties of Poly(urethane-isocyanurate) foam panels in relation with local chemical composition and morphology. *European Polymer Journal*, 2021, 163, pp.110899. 10.1016/j.eurpolymj.2021.110899 . hal-03465173

HAL Id: hal-03465173

<https://hal.science/hal-03465173>

Submitted on 16 Dec 2021

HAL is a multi-disciplinary open access archive for the deposit and dissemination of scientific research documents, whether they are published or not. The documents may come from teaching and research institutions in France or abroad, or from public or private research centers.

L'archive ouverte pluridisciplinaire **HAL**, est destinée au dépôt et à la diffusion de documents scientifiques de niveau recherche, publiés ou non, émanant des établissements d'enseignement et de recherche français ou étrangers, des laboratoires publics ou privés.

**Effect of surface curing temperature on depth-specific physical properties of
Poly(urethane-isocyanurate) foam panels
in relation with local chemical composition and morphology**

Joël Reignier^{1,2}, Françoise Méchin¹, Alexandru Sarbu³

¹ *Univ Lyon, INSA Lyon, CNRS, IMP UMR 5223, F-69621, Villeurbanne, France*

² Author to whom correspondence should be addressed. E-mail: joel.reignier@polymtl.ca

³ *SOPREMA, 67025, Strasbourg, France*

Published in *European Polymer Journal* vol. **163**, 110899 (2022)

Effect of surface curing temperature on depth-specific physical properties of Poly(urethane-isocyanurate) foam panels in relation with local chemical composition and morphology

Joël Reignier^{1,2}, Françoise Méchin¹, Alexandru Sarbu³

¹ Univ Lyon, INSA Lyon, CNRS, IMP UMR 5223, F-69621, Villeurbanne, France

² Author to whom correspondence should be addressed. E-mail: joel.reignier@polymtl.ca

³ SOPREMA, 67025, Strasbourg, France

ABSTRACT

Processing low density poly(urethane-isocyanurate) (PIR) rigid foam boards still remains challenging, especially for high thickness panels with the spontaneous formation of two-dimensional wrinkles. Increasing the double-belt conveyor's temperature (mold temperature in our case) was regarded as a way to increase the rigidity of the foam base material and, ultimately to increase the stiffness of the PIR foam under the facing. For that purpose, PIR foam samples simulating real panels were prepared at different mold temperatures and were chemically analyzed using ATR-FTIR spectroscopy while a Shore durometer (type OO) was used to estimate the foam rigidity in various locations of the model panel. Obviously, the isocyanurate content of the foam under the facing was found to increase with

the increase in mold temperature but surprisingly the Shore hardness demonstrated the reverse effect. This result was explained by the decrease in the density of the foam layer under the facing as the mold temperature increases, thereby counteracting the probable increase in stiffness of the foam base material itself. In addition, foam characterizations at different depths (rise direction) indicate that the chemical and mechanical gradients occurring in the first 20-30 mm tend to disappear as the mold temperature increases.

Keywords:

Polyurethane, polyisocyanurate, foam, infrared spectroscopy, Shore durometer, chemical gradients, density, mold temperature

1. Introduction

PIR foams panels (film substrate composite system) have been widely used for over 20 years and are relatively easy to produce for thicknesses lower than a dozen of centimeters. Nowadays, thicker panels are needed to meet new environmental standards but they often have surface defects (facing) in the form of wrinkles which appear during aging. For commercial insulation panels, these macroscopic surface defects can be considerable enough (highly notable defect amplitudes and/or wide area of the surface covered with 2D-wrinkles) that the customer might reject the merchandise or claim for a rebate. Aside from wrinkles observed in natural systems (aging of human skin or ripening fruits), wrinkles are now often encountered (mostly intentionally) in various artificial materials and devices (optical gratings, microfluidic devices) [1]. Basically, wrinkles form when an elastic bilayer composed of a stiff film bonded to a soft substrate is compressed beyond a critical strain (Figure 1) as defined by:

$$\varepsilon_c = \frac{1}{4} \left[3 \frac{(1-\nu_{film}^2)E_{substrate}}{(1-\nu_{substrate}^2)E_{film}} \right]^{2/3} \quad (1)$$

where ν and E are the Poisson ratio and the Young's modulus of the rigid film and the elastic substrate. The corresponding critical wavelength (λ_c) of the wrinkle pattern, dictated by the balance between the bending energy of the film and the stretching energy of the substrate, is theoretically determined by

$$\lambda_c = 2\pi h \left[\frac{(1-\nu_{substrate}^2)E_{film}}{3(1-\nu_{film}^2)E_{substrate}} \right]^{1/3} \quad (2)$$

where h is the thickness of the rigid film. Then the periodic wrinkles grow in amplitude with the applied strain. Observing the similarity of the wrinkling patterns of PIR foam insulation board facing with those reported in the literature for rigid film resting on a soft substrate, Reignier et al. [2] proposed to use these equations for PIR foam insulation boards in order to estimate the critical strain ($\epsilon_c \sim 0,5\%$) and the Young's modulus of the foam substrate (close to the facing) at the onset of wrinkle formation (from the measurement of λ).

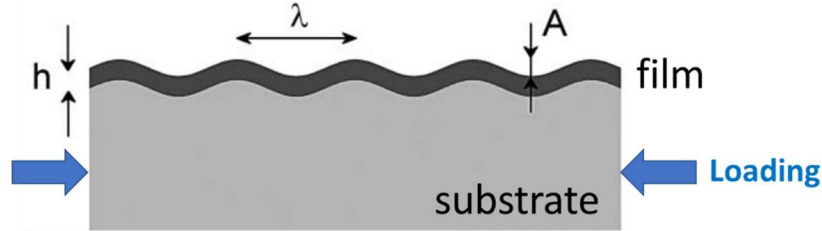


Figure 1. Schematic illustrating the geometry of wrinkles in an elastic thin film (thickness h) bonded to an infinitely thick elastic substrate. The wrinkles have a periodicity λ and amplitude A .

According to equation 1, the critical strain of wrinkle formation depends only on the material properties (the film and the substrate) and increasing the $E_{substrate}/E_{film}$ modulus ratio could allow to postpone the critical strain to a higher level and ideally beyond the real in-plane contraction occurring during aging. In theory, there would therefore be two different ways to increase the $E_{substrate}/E_{film}$ modulus ratio, either by increasing $E_{substrate}$ or by decreasing E_{film} . Unfortunately, this latter option is not favorable in our case because the foam in-plane shrinkage is strongly dependent on the mechanical

properties of the facing [2]: the lower the rigidity of the film (facing), the higher the shrinkage (ϵ) which would facilitate the formation of surface wrinkles. It was observed in practice for a given formulation and panel thickness that the amplitude of wrinkles increased as the mechanical properties of the facing decreased (internal work not published). Hence, the only possible solution (for a given facing) would be to increase the rigidity of the foam substrate close to the surface. The surface of PIR foam boards (right beneath the facing) was recently probed using a Shore durometer type OO and it was demonstrated that wrinkles are more prone to occur in the regions of low hardness [2]. The link between the cellular morphology under the surface (over a few millimeters) and the level of Shore hardness was clearly established: the more the elongated cell axis deviates from the rise direction, the lower the hardness. Apart from variation in the cell orientation which is intimately associated with the production line (process) and difficult to completely avoid, the question is how to increase the rigidity of the foam substrate? Obviously, increasing the density of the whole PIR insulation panel by adding less physical blowing agent should work, but at the expense of costs, application conditions and thermal conductivity. An alternative solution would be to increase the mechanical properties of the foam base material. It is often claimed in the scientific literature that the mechanical properties of PIR foams are directly controlled by the polymer matrix crosslink density. A typical example is given by the work of Modesti et al. [3] who studied the effect of isocyanate index of PIR foams and explained the increase in compression strength of the foam samples with the increase in isocyanate index from 200 to 250 by the increasing crosslink density that would render the polymer matrix more rigid. Surprisingly, the opposite trend was observed when the index was increased from 250 to 300 and the lower stiffness was then explained in terms of an excess in friability. In any case, care must be taken in interpreting these results with regards to the mechanical properties of the foam base material because data found in the literature are usually based on macroscopic measurements directly made on the foam, and other foam characteristics (density, cell shape factor, distribution of material between struts and walls...) may have changed at the same time. In addition, the friability tests (Abraser or Tumblin) often used to compare samples of different isocyanate indexes are one aspect of durability or

resistance to wear and tear, but do not give any information about compressive properties (elastic modulus and/or compressive strength at yield) [4].

To get more information about the relationship between the mechanical properties and the degree of crosslinking, it is necessary to take a close look at the domain of dense thermosets (non-foamed material). In that case, one of the main parameters is the glass transition temperature (T_g) of the thermosetting polymer with respect to the temperature at which the measurements of the mechanical properties are performed. On one hand, it is recognized that above T_g , the low-strain mechanical properties of thermosets can be approximated (in most cases) by the rubber elasticity theory (for an ideal rubber, the Poisson's ratio $\nu \rightarrow 0.5$). If a constant volume deformation is assumed for small strains, the equilibrium tensile modulus in the rubbery region (E_e) is then related to the inverse of the average molar mass between crosslink points (M_c) according to the following equation

$$E_e = 3\rho RT/M_c \quad (3)$$

where ρ is the density (kg/m^3) at the absolute temperature T (K) and R is the gas constant ($8.314 \text{ J.K}^{-1}.\text{mol}^{-1}$) [5]. Note that E_e is generally estimated at $T = T_g + 40^\circ\text{C}$. In other words, this relation implies that the elasticity modulus of the polymer networks in the rubbery state is almost independent of the molecular structure (scale of nanometers and monomers) and depends essentially on the macromolecular structure at a higher scale, i.e. the crosslink density ($1/M_c$) [5]. The lower M_c , the higher the crosslink density, the lower the molecular mobility and the higher the rigidity of the polymer. In the case of complete curing, compelling examples of this dependence can be found in the field of polymer gradient materials. For instance, bulk copolymerization of MDI with hydroxy-terminated polybutadiene rubber at various ratio between polyisocyanurate cycles (rigid crosslinking points) and flexible chain spacers gave crosslinked polyisocyanurate polymers with elastic modulus ($T_{\text{amb}} > T_g$) varying between 2.2 and 1960 MPa [6].

On the other hand, it is more difficult to make a coherent overview when the mechanical properties are determined at $T < T_g$ and this despite several studies available in the literature on elastic properties

of thermosets below T_g (mainly on amine-crosslinked epoxy resins). Aside from the fact that equation 3 is no longer valid, results may seem sometimes contradictory from one study to the other in part because the effect of crosslink density on mechanical properties is considerably less notable than above T_g . In some cases, the elastic properties of polymer networks in the glassy state were found to be practically independent of the crosslink density. For instance, it has been shown for epoxy-amine polymers that the elastic modulus and tensile strength at room temperature are independent of M_c between 375 and 1460 g/mol [7]. Shimbo et al. [8] demonstrated for acid-cured epoxy resins that the tensile strength was neither affected by the chemical composition nor by crosslink density for $T < T_g$. Lesser et al. [9] demonstrated from both tensile tests and storage moduli E' obtained from DMA measurements that the glassy moduli of amine-cured epoxy resins were independent of M_c ($380 \text{ g/mol} \leq M_c \leq 1790 \text{ g/mol}$). According to these authors, this result is typical of thermoset polymers because the small strains involved in modulus measurements are mainly controlled by local chain packing and stiffness which are not affected by higher length scale parameters like M_c [7, 10]. In other words, the motion of localized chain segments is not affected by the presence of crosslink points located many segments away [7]. Similarly, Crawford et al. [11] observed in the case of epoxy resins that quasi-static tensile modulus did not depend strongly on M_c or $T - T_g$ but they found that the tensile strength (that implies higher deformation levels) usually increases as M_c decreases. This latter trend is usually explained in terms of variations in T_g as a function of M_c based on the assumption that yield stress depends only on the temperature difference $T - T_g$ for networks of similar chemistry [12]. In the same vein, tensile strength vs $T - T_g$ curves of various M_c collapse reasonably well onto the same master curve, thus indicating that the only effect of M_c on yield strength is through a change in T_g [9]. This therefore indicates that the level of deformation applied during mechanical testing would play an important role in the glassy state ($T < T_g$). Another interpretation of the data indicates that the elastic modulus and yield stress of thermosetting polymers below T_g would depend on the molecular scale structure through the cohesive energy density (CED) which can be viewed as the whole energy of intermolecular interactions (Van der Waals forces) [10,13]. In this context, changes in volumetric

properties such as density are often used to interpret the evolution of mechanical properties as a function of crosslink density because higher densities are usually associated with higher intermolecular attractive forces (higher CED). Hence, the Young's modulus of epoxy networks in glassy state was found to increase almost linearly with the density [14,15,16]. Additional proof of that link was given by Rackley et al. [13] who prepared poly-*p*-divinylbenzene crosslinked polymers at different temperatures and pressures and demonstrated that the shear modulus (G) increased linearly with the density. However, care must be taken in the interpretation of the data because the variation of the hydrogen bonds concentration has a strong influence on the packing density and, as a result, greatly affects the CED [17]. In the end it is also interesting to note that despite huge differences in chemical structures, most polymeric materials (such as poly(methyl methacrylate), polystyrenes, polyamides, including aromatic amides, polyesters, polyimides, etc.) possess approximately the same Young's modulus in the glassy state with values varying within the range $2\text{-}3 \times 10^9$ Pa [18]. Even highly crosslinked polymer resins have modulus values never exceeding 6×10^9 Pa [14]. In consequence, changing the crosslinking density could only vary the modulus of elasticity of glassy polymer networks by a factor two or three at most, while E_e can vary by several orders of magnitude above T_g .

In our case, the matrix of PIR foam boards is supposedly made of highly cross-linked networks ($M_c \leq 1000$ g/mol) which are rigid at room temperature (T_{amb}) and thus should be characterized by glass transition temperatures well above ambient temperature ($T_g > T_{amb}$). As a result, the stiffness of the foam base material should not depend strongly on the crosslink density. A recent study on polyisocyanurate-based metal-foam composite elements brought up, however, new aspects that are somewhat encouraging [19]. These authors investigated the relation between isocyanurate content (estimated through ATR-FTIR spectroscopy measurements at different depths of the foam panel) and elastic properties of the polymeric matrix by performing nanoindentation tests on tiny foam fragments (at the scale of cell struts) embedded in a thermoset epoxy resin. They demonstrated that the Young's modulus of the foam base material increases from 3.6 GPa (surface) to 3.93 GPa (core) along with the increase of the isocyanurate/urethane ratio (peak area ratio: A_{1405}/A_{1420}) from 0.52 to 2.02. Even if the

maximum difference of Young's modulus was only of $\Delta E \sim +15\%$, the tendency was clearly established and moves in the right direction. The increase in matrix stiffness with increasing isocyanurate content was explained by the higher temperature occurring in the core of the foam with respect to the surface. In addition, the images of the foam struts, directly observed by atomic force microscopy (AFM) revealed that the foam struts near the cover layers (metal sheet) are more uniform than the structure observed at a depth of 30 mm. According to the authors, the coarser segregations observed in the latter case may correspond to the accumulations of the individual PIR/PUR components. However, the authors have not compared the mechanical properties of the various foams, which would have permitted to draw a direct link between the mechanical properties of the foam and its base material. Transposing their results into our studies, one would reasonably expect that increasing the proportion of isocyanurate on the surface of PIR foam panels by increasing the surface temperature may increase not only the rigidity of the base material, but also that of the foam close to the surface (under the facing), giving a chance to impede the formation of surface wrinkles. Given the impossibility of extensively changing the temperature of the double-belt conveyor (production line) and the need to be able to characterize the foam from both a mechanical and a chemical point of view, it was decided to conduct this study using a batch process (at a smaller scale) in a laboratory, using a home-made temperature-controlled heating mold (SI1). Particular attention was paid to the characteristics of the foam surface in contact with the facing, but measurements were also taken throughout the entire thickness of the foams (rise direction) in order to figure out the impact of the surface temperature on various chemical and/or physical parameters throughout the thickness of the foam panel.

2. Experimental details

2.1. PIR Foam Preparation

The PIR foam buns (isocyanate index = 300) were produced in our laboratory and were obtained through a reactive foaming process with polymeric methylene bis(phenyl isocyanate) (pMDI) and a

polyester polyol using both water and isopentane as chemical and physical blowing agents, respectively. Two different kinds of catalysts, namely a tertiary amine and an alkali metal carboxylate were used to promote blowing and gelling reactions as well as the trimerization of pMDI. The exact details of the formulation are not given for confidentiality reasons. It must be pointed out that all the work described herein was done using the same formulation, and the effects observed are thus related only to the various mold temperature. The materials were mechanically mixed together and poured into a 25 cm x 25 cm aluminum mold measuring 15 cm in height and set at different temperatures. Only the bottom part of the mold possessed a heating resistor (attached under the aluminum bottom plate) which is connected to an electrical temperature control system (SI1). The 4 lateral faces of the mold were not specifically heated but it was observed that their temperature increased as the setting temperature of the bottom plate was increased, because of the metal-to-metal contact with the heated bottom plate. Note that samples taken for the various analyses were only taken in the central part of the foam bun, so as to not be influenced by the lateral sides of the mold. The bottom face of the mold was covered with a gas-tight facing typically used in foam insulation boards for setting temperatures up to $T_{\text{mold}}=120^{\circ}\text{C}$. Higher temperatures cause thermal degradation and delamination of the multi-layer film, so it was replaced with a more heat resistant aluminum foil for $T_{\text{mold}}>120^{\circ}\text{C}$. Each foam block was removed from the mold after 15 min, allowed to cooldown freely at room temperature and aged for a time period varying from $t\sim 1$ h to $t\sim 4500$ h (the precise moment when the isocyanate is added and mixed with polyol premix is considered as the starting time).

It is essential to mention that the mold was open at the top to allow the foam to rise and expand freely. This should ensure that cells are elongated in the rise direction, in particular those close to the facing, necessary condition for having a chance to detect a change in the rigidity of the PIR matrix by measuring the mechanical properties of the foam. In return, the use of only one facing would prevent the formation of 2D-wrinkles because the lateral shrinkage of the foam will be higher on the side opposite to the facing which will tend to slightly stretch the facing. In other words, it was not possible to visually compare the effect of T_{mold} on the formation of 2D-wrinkles with our experimental device

but it is hoped that such an approach will provide valuable information regarding the effect of the double-belt temperature on the formation of 2D-wrinkles in PIR insulation foam panels.

2.2. Kinetics of Foam Formation

The reactivity of foam formation is traditionally followed by the physical change of the properties such as “cream time” (t_{cream}), “gel time” (t_{gel}) and “tack-free time” ($t_{\text{tack-free}}$). The cream time corresponds to the start of bubble rise, due to the gas reaction. The gel time corresponds roughly to the starting point of stable crosslinked network formation. In the case of PIR formulation, it corresponds to the time when a flat wooden applicator stick encounters resistance when it is pushed into the foam bun. At the tack-free time, the outer surface of the foam loses its stickiness, and it represents the end of the macroscopic chemical and physical phenomena. The characteristic times of our base formulation were estimated in a plastic cup without any heating system and are reported in Table 1. In our case, the end of rise time (t_{rise}) corresponds to the end of the maximum expansion phase of the foam and can be roughly estimate by $t_{\text{tack-free}}$.

Table 1: Characteristic times of the PIR foam

Cream time (s)	Gel time (s)	Tack-Free time (s)
13 ± 2	60 ± 4	160 ± 10

2.3. ATR-FTIR Spectroscopic Characterizations

Fourier Transform Infrared Spectroscopy (FTIR model: Thermo Scientific Nicolet iS10 spectrometer) was used in attenuated total reflectance mode (ATR) in the range $4000\text{-}600\text{ cm}^{-1}$ (resolution 4 cm^{-1}) to characterize the chemical structure of the various foam samples. Using these parameters, the minimum peak interval that can be distinguished (“data spacing”) was approximately 0.48 cm^{-1} . For chemical gradient studies (section 3.2), a square base foam column (around $2\text{ cm} \times 2\text{ cm}$) with the long axis parallel to the foam rise direction (z-axis) was taken in the center of each foam bun (each one

corresponding to a given T_{mold}) and then was sliced in approximately 5 mm layers using a razor blade, as the spectroscopy measurements were carried out. It is worth mentioning that the clamping force (pressure) used to ensure tight adhesion between the sample and the ATR prism was strong enough to crush the foam layer by a factor about $\times 10$, giving an almost bulky film with a thickness of around 0.5 mm. All spectra were analyzed with OMNIC Spectra software with ATR correction. All measurements were done at room temperature ($23 \pm 2^\circ\text{C}$).

2.4. Shore OO Durometer Measurements

The hardness of the foam samples in the rise direction was estimated using a handheld Shore durometer (type OO, Hildebrand model HD 3000). This test method was found to be very effective to probe the surface of PIR foams [2] because it can be applied quickly to small specimens having just two parallel flat surfaces and a minimum thickness of 6 mm (ASTM D2240). Each individual reading gives a dimensionless value comprised between 0 and 100 (higher values indicating a harder material). To avoid interference between measurements, each indentation must be done at a distance of at least one indenter diameter (i.e. 2.38 mm) away from other indentation marks. The time is measured from the moment when the liquid mixture is poured into the mold ($t=0$ s). Each data point corresponds to the average of 5 measurements. The repeatability of Shore hardness measurements can be reasonably estimated at about ± 1 .

2.5. Foam Density Measurements

The (apparent) density of the closed-cell foam specimens was simply determined at room temperature as the ratio of its weight and volume. Foam samples of the different foam layers (depth of 5 mm) were cut using a razor blade at ambient temperature. The dimensions used to calculate the volume of each sample were determined using a calliper. The weight of each sample was determined using scales with a resolution of 10^{-5} g. The repeatability of the density measurements can be reasonably estimated to about $\pm 5\%$.

2.6. Morphology observation and image analysis

Foam samples fractured in liquid nitrogen were coated with gold and observed perpendicularly to the rise direction using a scanning electron microscope (SEM) (Hitachi, model S3500N) operated at a 15 kV voltage. A semi-automatic method of image analysis (ImageJ software, U.S. National Institutes of Health) was used to quantify the cellular morphology. The average cell size is given by the projected area diameter ($d_A=[4A/\pi]^{1/2}$, where A is the projected area). The average cell shape is given by the Feret aspect ratio ($FeretAR=MaxFeret/MinFeret$) where MaxFeret (MinFeret, respectively) is the longest (shortest, respectively) distance between any two points along the cell boundary. The cell orientation is characterized by the angle (θ) between the maximum caliper diameter (MaxFeret) and a line perpendicular to the thickness direction (z-axis). An average number of about 150 cells was used to evaluate cell size, orientation and aspect ratio for each data point reported in Figure 18. The cell population density, as defined by the number of cells per unit volume of the original non-foamed polymer, was evaluated using the following equation:

$$\beta \cong \frac{6 \times 10^{+12} [(\rho_{polymer}/\rho_{foam}) - 1]}{\pi d^3} \quad (4)$$

where β is the cell population density (cells/cm³), d the average diameter of the cells (μm); $\rho_{polymer}$ and ρ_{foam} the densities of the non-foamed and foamed polymers, respectively (g/cm³).

3. Results and discussion

3.1. Effect of mold temperature on the surface chemistry at $t \sim 1$ h

3.1.1. Evolution of the C-N stretching vibration ($1350\text{-}1450\text{ cm}^{-1}$) of isocyanurate ring as a function of mold temperature at $t \sim 1$ h and $t \sim 4500$ h

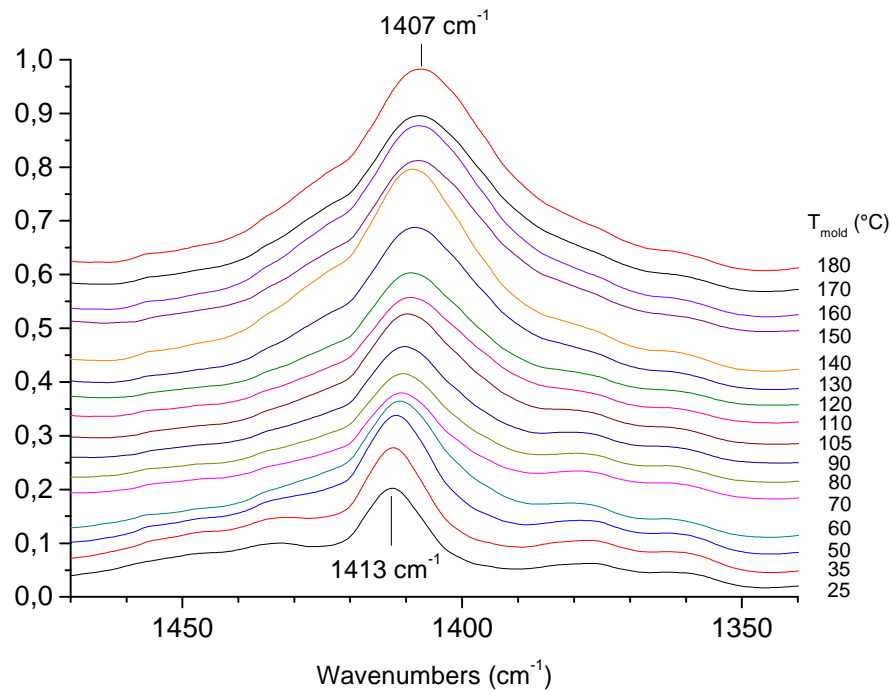


Figure 2: ATR-FTIR spectra of the PIR foam surface (after facing removal) as a function of mold temperature (°C) in the range $1340\text{-}1470\text{ cm}^{-1}$ corresponding to the C-N stretching vibration of isocyanurate ring for $t \sim 1$ h.

The product of the isocyanate trimerization, namely the isocyanurate ring, was followed using the C-N stretching band in the 1410 cm^{-1} region [20,21,22,23]. The data plotted in Figure 2 suggest that the intensity of the C-N stretching of the isocyanurate peak (1410 cm^{-1}) increases as the mold temperature increases which is consistent with the view that the isocyanurate reaction yield is controlled by the temperature. To best quantify the variation of a given reaction product, it is common to normalize all

spectra with the absorbance of a given species (the C=C stretching vibration of the phenyl peak at 1595 cm^{-1} in our case) which should not depend on the extent of the various reactions [24]. In addition, it is worth mentioning that the height for each peak of interest was measured with respect to a baseline connecting the lower points on either side of the peak (a zone where the absorbance is low). The anchor points were chosen at 1350 cm^{-1} and 1470 cm^{-1} for the C-N stretching of isocyanurate, and at 1565 cm^{-1} and 1630 cm^{-1} for the C=C stretching vibration of the aromatic ring (phenyl), respectively. By proceeding on this basis, Figure 3 indicates that the content of isocyanurate at the surface (under the facing) increases as a function of mold temperature and tends to level off beyond a mold temperature of about 160°C .

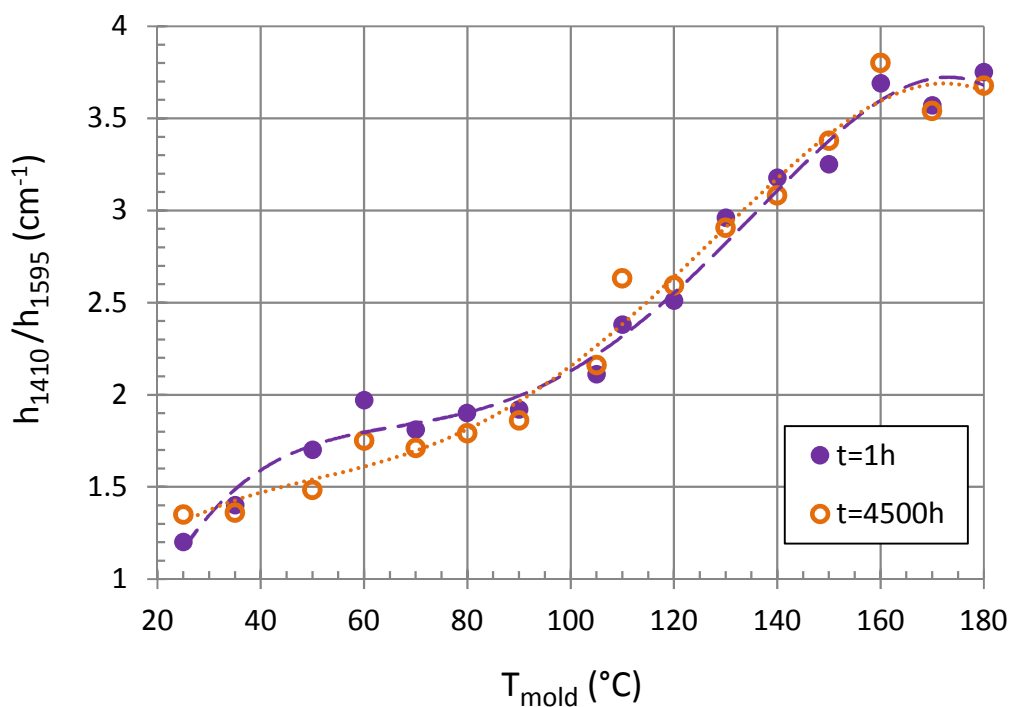


Figure 3: Effect of mold temperature on the h_{1410}/h_{1595} (isocyanurate/phenyl) peak height ratio for the surface (under the facing) at $t\sim 1\text{ h}$ and $t\sim 4500\text{ h}$. The lines are only guides for the eyes.

In addition, Figure 2 shows that the peak maximum wavenumber (often called “peak position”) is not constant. For $t\sim 1\text{ h}$, its position progressively decreases from about 1413 cm^{-1} to about 1407 cm^{-1} as

the surface temperature increases from 25 to 180°C, as shown in Figure 4. The evolution of isocyanurate content as a function of depth in PIR foam insulation panels taken from the European market was recently studied. It showed a similar downwards frequency shift of the C-N stretching vibration of the isocyanurate ring that was shown to be related to the increase in isocyanurate content from the surface to the core [25]. In the same way, Figure 4 reveals a linear decrease (correlation coefficient $R^2 > 0.98$) in the peak maximum frequency, but in this case as the mold temperature increases. This result clearly indicates that the proportion of isocyanurate at the surface increases with the increase in mold temperature.

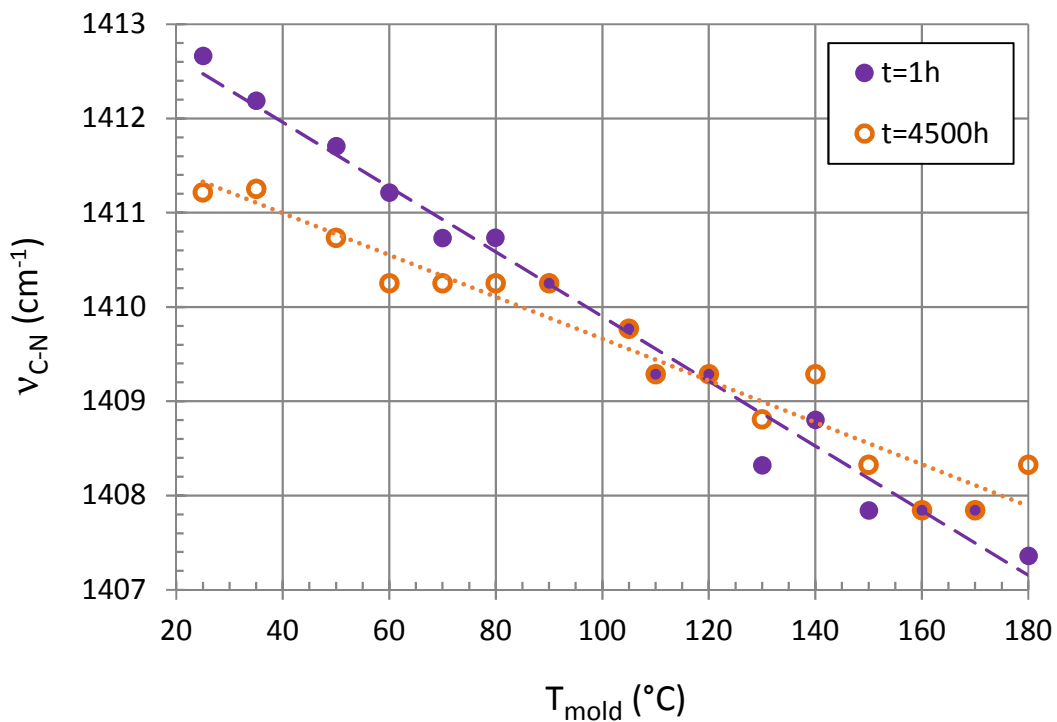


Figure 4: Effect of mold temperature on the maximum intensity position (wavenumber) of the C-N stretching vibration of isocyanurate (peak maximum) for the surface (under the facing) at t~1 h and t~4500 h. The dashed line (t~1 h) and dotted line (t~4500 h) correspond to the best-fit line through all the data points with a linear regression ($R^2 \sim 0.98$ and $R^2 \sim 0.93$, respectively).

To better understand what is happening, the typical evolutions of the degree of conversion and of the

glass transition temperature during the processing of thermosetting polymers will be described. Basically, the glass transition temperature (T_g) of a thermosetting mixture should increase during polymerization from its initial value (often called T_{g0}) which is generally below room temperature (reactants are liquid at $T_{g0} < T < T_{amb}$) until it reaches the curing temperature (T_c). At this particular moment, molecular relaxation times become very large because of the vitrification phenomenon and as a result, the polymerization is strongly slowed down or even almost completely stopped and the chemical reactions are at that point controlled by diffusion. In the case of epoxy resins, T_g was found to exceed T_c to a maximum of about 20-30°C if the curing time was long enough [26,10]. In addition, the T_g of thermosets was found to increase linearly with their crosslink density ($1/M_c$) [27,5]. However, when expressed as a function of the degree of conversion (α), it was established that the increase in T_g ($dT_g/d\alpha$ slope) was greater at higher degrees of conversion [28,29,15]. In our case, the cure cycle mainly takes place in a heated open mold (T_w) for $t \sim 15$ min followed by demolding and aging at room temperature for various times. After demolding, the surface temperature of the foam formerly in contact with the heating element quickly cools down and therefore no significant increase in the amount of trimer at the foam surface is to be expected after $t_c \sim 15$ min. Indeed, only an increase in temperature beyond the initial curing temperature could theoretically restart the trimerization process and could further raise the degree of conversion [10]. From all the above it thus appears that the mold temperature is the main parameter that would control the conversion of the PIR foam at the surface: the higher T_{mold} , the higher the isocyanurate level. Carleton et al. [30] demonstrated for dense composites based on polyisocyanurate polymers and glass strand mat that both the T_g and trimer conversion increased with the mold temperature. In addition, they demonstrated that the state of cure, as probed by the T_g , was related to the maximum exotherm obtained during reaction and the duration of that exotherm as well. According to these authors, the primary variables affecting cure are the catalyst level, which is constant in our case, mold temperature (our main variable), in-mold time ($t_c \sim 15$ min in our case) and post-curing. The latter was replaced in our case with ageing at room temperature.

In a previous work, it was demonstrated for PIR foam boards probed at different depths that there was a direct relationship between the C-N frequency of isocyanurate ring and the h_{1410}/h_{1595} peak height ratio [25]. It was suggested that the decrease of $\nu_{\text{isocyanurate}}$ (frequency peak maximum) was related to the reduction of the concentration of H-bonding between N-H and C=O (isocyanurate) as the trimer content increased. Indeed, chemical crosslinks are believed to reduce molecular mobility with respect to a non-reticulated analog because of the occurrence of geometrical constraints [5] which should hamper the formation of noncovalent interactions between macromolecules [31]. In the present case, Figure 5 combines the data from Figures 3 and 4 and coherently demonstrates that this link prevails in the case of foam surfaces processed at different T_{mold} .

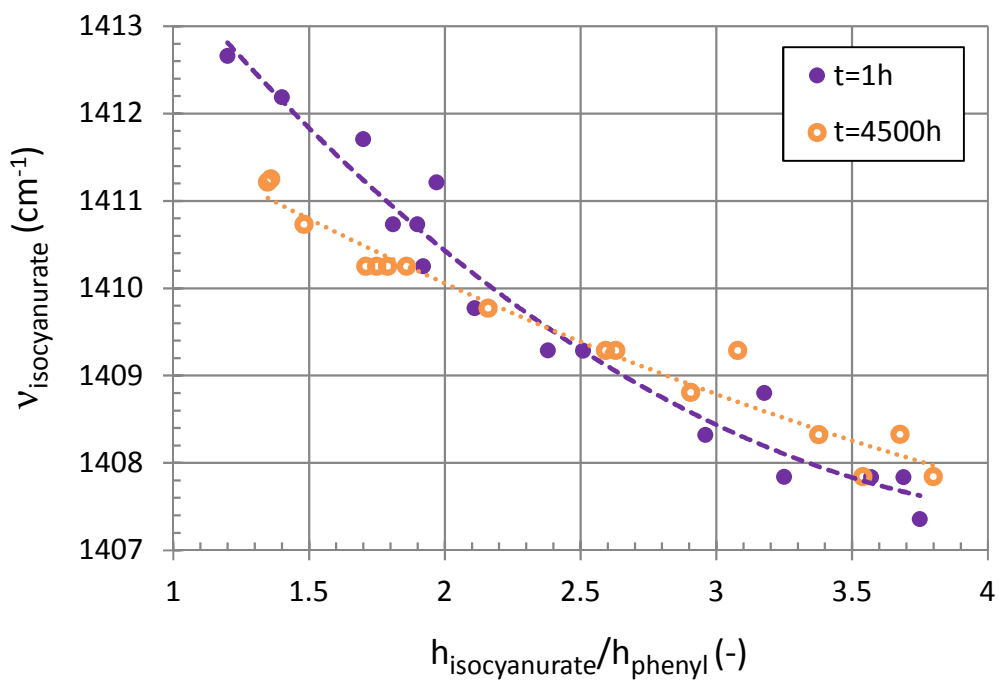


Figure 5: Evolution of C-N frequency of isocyanurate ring (peak maximum) as a function of isocyanurate/phenyl (h_{1410}/h_{1595}) height ratio for all PIR foam samples at $t \sim 1$ h and $t \sim 4500$ h. The lines are only guides for the eyes.

Using the intensity of the peak at 1220 cm^{-1} (C-O bond stretching) to estimate the proportion of

urethane (with anchor points between 1160 cm^{-1} and 1345 cm^{-1}), Figure 6 reveals the decrease in the h_{1220}/h_{1410} (urethane/isocyanurate) peak height ratio with the increase of T_{mold} at $t\sim 1\text{ h}$. The major effect occurs between T_{amb} and about $60\text{-}80^\circ\text{C}$ beyond which the urethane/isocyanurate proportion tends to level off. The higher mold temperature seems to promote the formation of isocyanurate, which may be explained by the higher activation energy of isocyanurate with respect to urethane formation. Similar urethane/isocyanurate gradients have been reported recently for industrial PIR foam insulation panels with metal facing [19] and flexible facing [25].

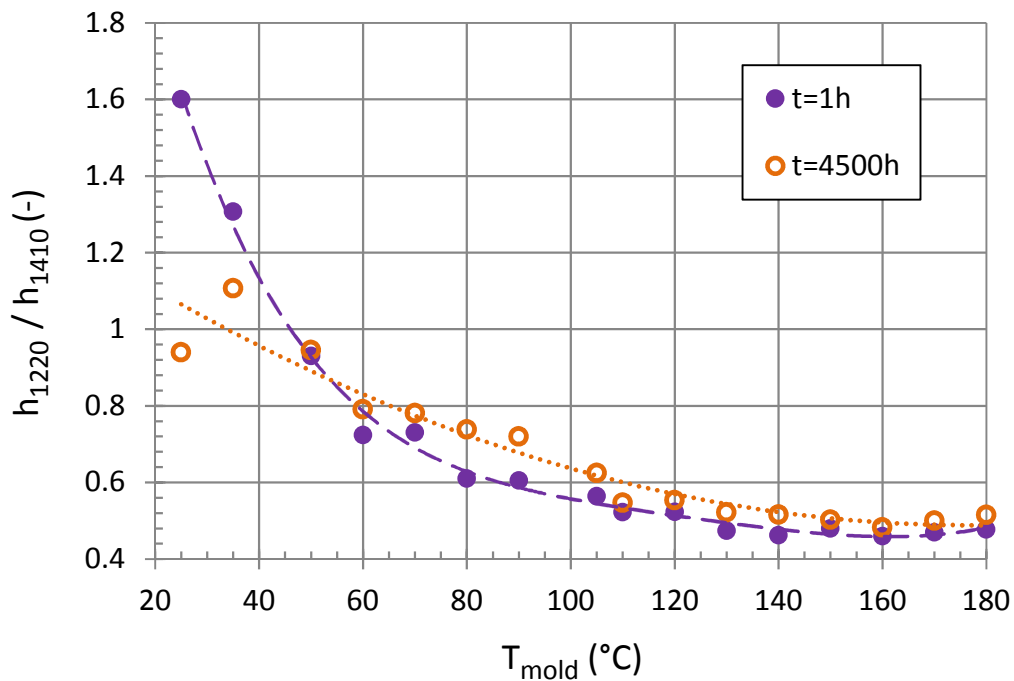


Figure 6: Effect of mold temperature on the evolution of the urethane/isocyanurate ratio (as probed by the h_{1220}/h_{1410} peak height ratio) for the surface (under the facing) at $t\sim 1\text{ h}$ and $t\sim 4500\text{ h}$. The lines are only guides for the eyes.

Figures 3 and 4 also show the level of trimerization at $t\sim 4500\text{ h}$ for comparison purpose. The decrease in the isocyanurate peak maximum ($\nu_{\text{C-N}}$) with aging can clearly be seen in Figure 4 for temperatures lower than approximately 90°C . Based on our previous work [25], this would indicate that the

isocyanurate content increased between $t \sim 1$ h and $t \sim 4500$ h. However, this “supposed” increase in isocyanurate content is not visible in Figure 3 where the values of h_{1410}/h_{1595} peak height ratio even have the tendency to be slightly lower between 40°C and 80°C. Both information elements seem to be contradictory and one may ask whether the proportion of isocyanurate really changes during aging at room temperature? On one side, the isocyanurate ring is recognized as thermolytically and hydrolytically stable and as a result is not expected to degrade during aging at room temperature [32]. On the other side, it is therefore very unlikely that the proportion of isocyanurate at the surface increases beyond the value obtained at $t \sim 1$ h during aging at room temperature. This suggests that the decrease of the isocyanurate peak maximum (v_{C-N}) observed at $t \sim 4500$ h (with respect to $t \sim 1$ h) is not related to the real increase of isocyanurate content but rather to the decrease in the concentration of H-bonding between the N-H group of urethanes and the C=O group of the isocyanurate ring during aging. Here are different possible scenarios which could feed this assumption: (i) The lower relative proportion of urethane (h_{1220}/h_{1410}), the N-H provider, reported in Figure 6 at $t \sim 4500$ h for temperatures below 50°C would go in this direction although it is hard to believe that thermal degradation of urethane groups can occur at room temperature. Reaction of urethane with residual -NCO, still present in vast amounts at low T_{mold} after $t \sim 1$ h, to form allophanate could potentially reduce the amount of urethane groups and are discussed in the section 3.1.2. (ii) Physical aging, which is rarely discussed in the case of PIR foam panels, could also play a role in decreasing H-bonding because the major difference between the two curves reported in Figure 4 appears at low isocyanurate content and it is recognized that physical aging is more prone to occur when the crosslink density is low [33]. This effect may, however, be wholly or partly counterbalanced by the higher proportion of hydrogen bonds found at low isocyanurate content which could slow the relaxation process [34,35]. (iii) Another possible explanation for the observed trend may be related to the absorption of water molecules (from outside air) which may potentially disrupt the existing hydrogen bonds [36]. It must be pointed out however that the water molecules diffusing from the unprotected part of the foam bun can also react easily with free isocyanate groups to form urea (see the next section for a detailed analysis of the

variation of free isocyanate as a function of T_{mold}).

3.1.2. Evolution of unreacted isocyanate ($R-N=C=O$) as a function of mold temperature at $t \sim 1$ h and $t \sim 4500$ h

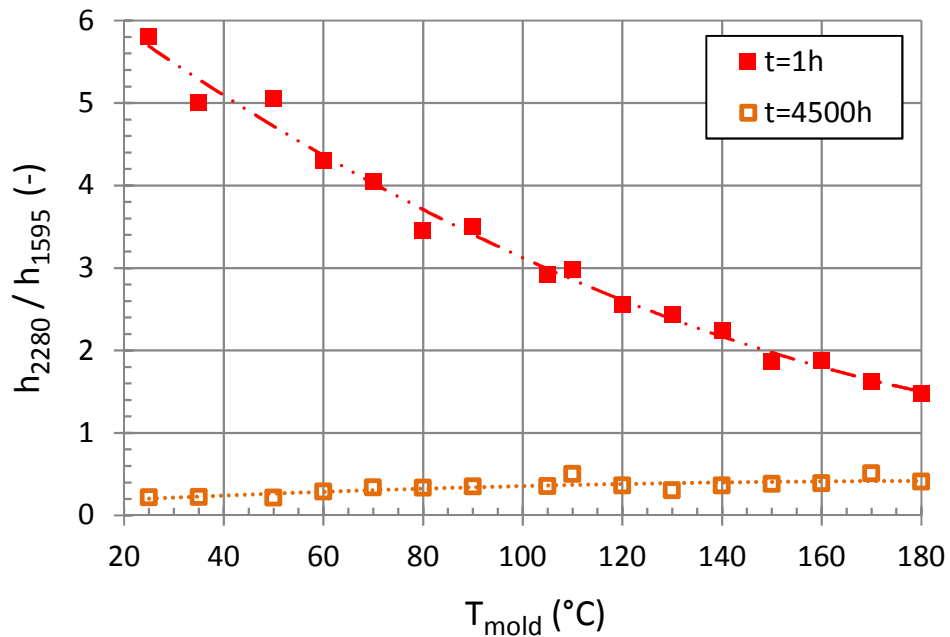


Figure 7: Effect of mold temperature on the h_{2280}/h_{1595} (isocyanate/phenyl) peak height ratio for the surface (under the facing) at $t \sim 1$ h and $t \sim 4500$ h. The line are only guides for the eyes.

Isocyanurate ring results from the cyclization of three isocyanate groups and a lower concentration of isocyanate groups may be expected with increasing isocyanurate concentration. The infrared band of unreacted $-N=C=O$ functions (asymmetric stretching vibration) was found around 2280 cm^{-1} in our PIR foams. The h_{2280}/h_{1595} (isocyanate/phenyl) peak height ratio for the surface (under the facing, i.e. $z=0$ mm) decreases as the mold temperature increases (at $t \sim 1$ h), as shown in Figure 7. Finding unreacted $-NCO$ functions was expected, even at high mold temperatures. Indeed, several authors [37,38,3,22] demonstrated that the isocyanurate yield (as defined by the proportion of NCO groups theoretically available at the end of the reactions with OH and amine, and which have effectively

reacted to form isocyanurate) for PIR foams of various index is never 100%. To get an idea of the order of magnitude, Priester et al. [22] demonstrated for PIR foams with isocyanate index of 350 (50/50 mol.% H₂O/CFC-11 blown) and 450 (100% CFC-11 blown) that about 30% of the isocyanate remained unreacted after 100 min. Even if the isocyanurate content increased when the NCO index increased [39], it was found that the final degree of isocyanate conversion into isocyanurate decreased with increasing isocyanate index. This phenomenon was explained by the restricted mobility of -NCO groups as the density of cross-linkages increases, preventing complete reaction [37,38,3,40]. In our case, however, the index is constant regardless of the mold temperature (as a reminder, the same formulation was used in all cases) and the decrease of the isocyanate peak intensity observed at the surface (after 1 h) when the mold temperature rises is consistent with the increase of isocyanurate content reported in Figures 3 and 4. The direct linear relation (correlation coefficient R²=0.96) between the isocyanate content (as probed by the h_{isocyanate}/h_{phenyl} peak height ratio) and the C-N frequency of isocyanurate ring (peak maximum) reported in Figure 8 (at t~1 h) may be taken as additional evidence. This line of reasoning implies that -NCO groups react at first with NH and OH groups while allophanate, biuret and isocyanurate groups are generated in a second phase. Špirková et al. [41] studied the reaction of excess phenyl isocyanate with 1-butanol (in 1,4-dioxane and in bulk) in the presence of dibutyltin dilaurate (catalyst) at temperatures of 90 and 120°C and underlined that under those conditions, the urethane formation is too fast to determine its rate constant with respect to the formation of allophanate and biuret. In the case of PIR rigid foams (index 350) blown with a mix of CFC-11 and water (50/50 mol%), Priester et al. [22] observed that the urethane formation started immediately after mixing while the onset of isocyanurate only appeared after 3 min. Al Nabulsi et al. [42] mimicked the complex reactions of PIR foam formulations (isocyanate index 350) by mixing *p*-tolyl isocyanate (*p*TI) with diethylene glycol methyl ether (DEME) (at a fixed molar ratio of 3.5:1) in propylene carbonate as solvent and at constant temperature of 70°C. Comparing the kinetics obtained for potassium acetate (KOAc) and potassium trifluoroacetate (KOAc^F) catalysts of different nucleophilicity, they demonstrated by *in situ* IR spectroscopy that the product of reactions, namely

carbamate (urethane) and isocyanurate were obtained at the same molar ratio for both catalysts. This finding suggests that the isocyanate reacted preferentially with the alcohol (to generate carbamate) and only after that the remaining isocyanate trimerized to isocyanurate. But it should be stressed that side reactions, ubiquitous in urethane and isocyanurate chemistry, would certainly disrupt this simplified scheme.

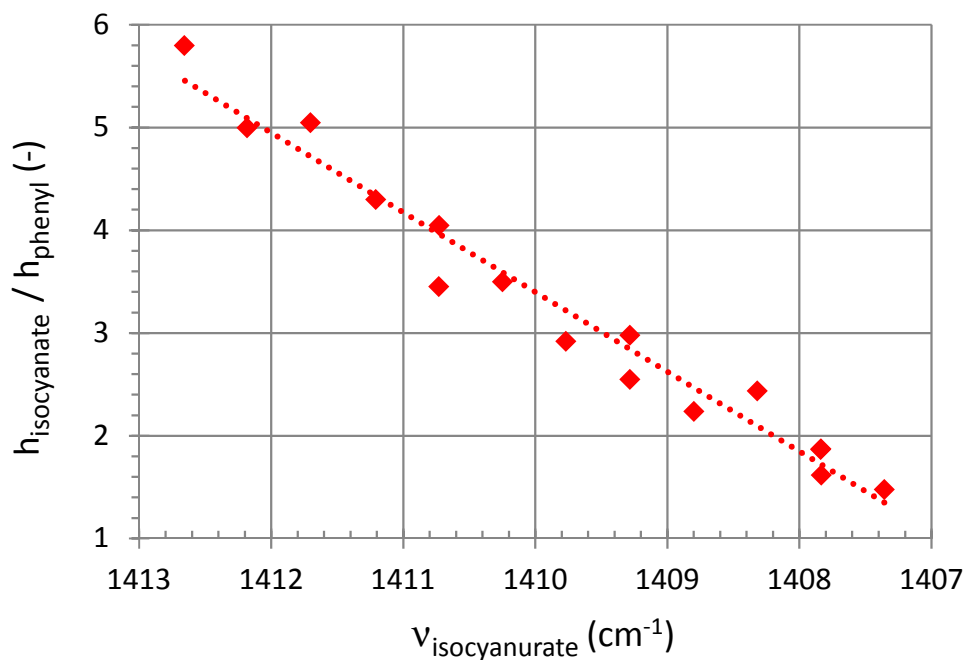


Figure 8: Evolution of isocyanate/phenyl (h_{2280}/h_{1595}) height ratio as a function of C-N frequency of isocyanurate ring (peak maximum) for all PIR foam samples at $t \sim 1\text{h}$ (surface). Note that the isocyanurate content simultaneously increases from the left to the right (reversed scale). The dotted line corresponds to the best-fit line through all the data points with a linear regression ($R^2=0.96$).

It is worth noting that the level of unreacted isocyanate at the surface, with an average value of $h_{2280}/h_{1595} \sim 0.3 \pm 0.03$, becomes very small after a period of about 4500 h and does not seem to depend on the mold temperature anymore, as shown in Figure 7. Indeed, the evolution of the h_{2280}/h_{1595} (isocyanate/phenyl) peak height ratio (on surface) reported in SI2 as a function of time and for the

different T_{mold} demonstrates that all curves merge to form a common curve for long periods of times regardless of the initial level of isocyanate. This result means that the vast majority of residual -NCO still present after 1 h have been consumed during aging at room temperature for $t \sim 4500$ h and it seems reasonable to ask ourselves what those NCO groups became. (i) The first hypothesis regarding the residual -NCO consumption during aging at room temperature is the formation of urea groups. Indeed, residual -NCO groups can react with atmospheric humidity, leading to an amine group. This latter can potentially condense with an additional isocyanate from the vicinity, leading to a urea linkage. This was indeed the main conclusion of a solid-state NMR study by Duff et al. [32] on a ground MDI-based polyisocyanurate network aged for about 7 months at room temperature under ambient atmosphere (25-50% RH). In addition, the authors indicated that air-exposed samples did not show any significant further reaction of urea linkages with isocyanate groups to form biuret, which may be linked to the difficulty of urea group to meet remaining isocyanate end group. In the case of polyurethane cast elastomers ($T_{\text{amb}} > T_g$) prepared with only a small excess of -NCO (index 110), Prisacariu et al. [43] demonstrated that the enhancement of mechanical properties during aging at room temperature ($T=25^\circ\text{C}$; 50% RH) was mainly due to the formation of urea groups (by the increase of hydrogen bonds). (ii) The second hypothesis regarding the residual -NCO consumption during aging at room temperature is the formation of allophanate group. In contrast to the formation of urea, this reaction does not require the presence of water molecules diffusing from atmospheric air but only reaction between urethane group and unreacted -NCO group. Allophanate could subsequently react with another residual -NCO group, leading to stable isocyanurate. One of the main issues is to determine whether the formation of allophanate and the subsequent reactions with NCO groups could occur at room temperature. According to Šebenik et al. [44], the formation of allophanate crosslinking in bulk is favored in the 130-140°C temperature range for low-catalyzed systems. Similarly, Ionescu [45] explained that without catalyst, allophanate formation needs temperatures greater than 110°C because isocyanate has a much lower reactivity with urethane groups than with amine group, primary and secondary hydroxyl groups or water. Heintz et al. [46] studied the effect of temperature on side

reactions during the formation of polyurethane prepolymer based on poly(propylene glycol) and MDI (NCO/OH=1.61) and demonstrated that without catalyst, the amount of branches arising from allophanate linkages was negligible at temperature of $T=108^{\circ}\text{C}$ (only 0.6 % of nitrogen atoms were engaged in allophanate after 1 h) while the amount reached 10% after 3h at 145°C . Kogon [47] found that ethyl α,γ -diaryl allophanate could be generated in good yield at room temperature from the reaction of aryl isocyanate with ethyl N-phenylurethane (mineral spirit was used as a solvent) in presence of metal carboxylate as catalyst. In the same study than that previously cited, Al Nabulsi et al. [42] followed by in situ NMR spectroscopy (using deuterated dimethyl sulfoxide as a solvent) the formation of isocyanurate at 25°C in presence of alcohol at a molar ratio of 3.5:1:0.002 (TI:DEME:KOAc^F) and demonstrated that the formation of isocyanurate only started once the allophanate reached a critical concentration of 8% molar ratio. In addition, three consecutive phases were distinguished, namely the carbamate phase, the allophanate phase and the isocyanurate phase. In the latter case, urethane concentration was found to increase as much as the isocyanurate increase because of the regeneration of starting alcohol during formation of isocyanurate from allophanate. From the above it appears that numerous factors (type and concentration of catalysts, presence of solvent or bulk polymerization, temperature range...) could affect the formation of allophanate but it would seem that allophanate formation would be precluded at room temperature in the absence of any solvent (bulk polymerization), even in presence of the appropriate catalyst.

In our case, on one side the gas-tight facing should prevent water molecules from directly diffusing on the tested surface of the foam, but atmospheric humidity may still diffuse slowly from the unprotected lateral face of the foam bun, leading to the formation of urea groups. Even if the PIR matrix is in the glassy state at room temperature ($T_{\text{amb}} < T_g$), water molecules should still be free to diffuse through the solid PIR foam to react with residual -NCO. On the other side, even if the presence of allophanate that has not yet reacted with residual -NCO (to form isocyanurate) is expected at the end of cure for the highest T_{mold} (surface), this does not mean that additional allophanate could be generated during the aging period at room temperature. Allophanate group formation requires the “encounter” between

urethane and -NCO end group, both of them having a limited mobility inside our 3D glassy polymer network, but could be facilitated at low T_{mold} where the proportion of residual -NCO is maximum and the surface T_g presumably lower. Unfortunately, the detailed analysis of IR spectra has not allowed the quantification of each reaction separately because the carbonyl stretching vibration of urea linkage (C=O) coincides with the strong and broad absorption envelope located between 1620 and 1760 cm^{-1} which encompasses not only the carbonyl bands of urethane (free and H-bonded) and isocyanurate, but also the C=O stretching vibrations of allophanate.

3.2. Chemical and Physical Gradients at $t \sim 4500$ h

3.2.1. Evolution of isocyanurate content as a function of depth for the various mold temperatures ($t \sim 4500$ h)

The various foam samples were analyzed by FTIR-ATR after an aging period of around 4500 h at ambient temperature and the results corresponding to the different layers from the surface to a depth of 60 mm are reported in Figure 9. As expected, the isocyanurate/phenyl peak height ratio of PIR foams increases from the surface toward the inside of the foam. All $h_{1410}/h_{1595}=f(z)$ curves converge to the average value of about 4.51 ± 0.08 (-) (for $55 \geq z \geq 60$ mm) which indicates that the isocyanurate level is maximum in the core where it does not depend, at first glance, on the initial surface temperature (T_{mold}). The chemical gradients typically spread over a 20-30 mm but can reach a depth as high as 45 mm in the least favorable case ($T_{\text{mold}} \sim 20^\circ\text{C}$) while it reduces to only 5 mm for $T_{\text{mold}} \geq 160^\circ\text{C}$.

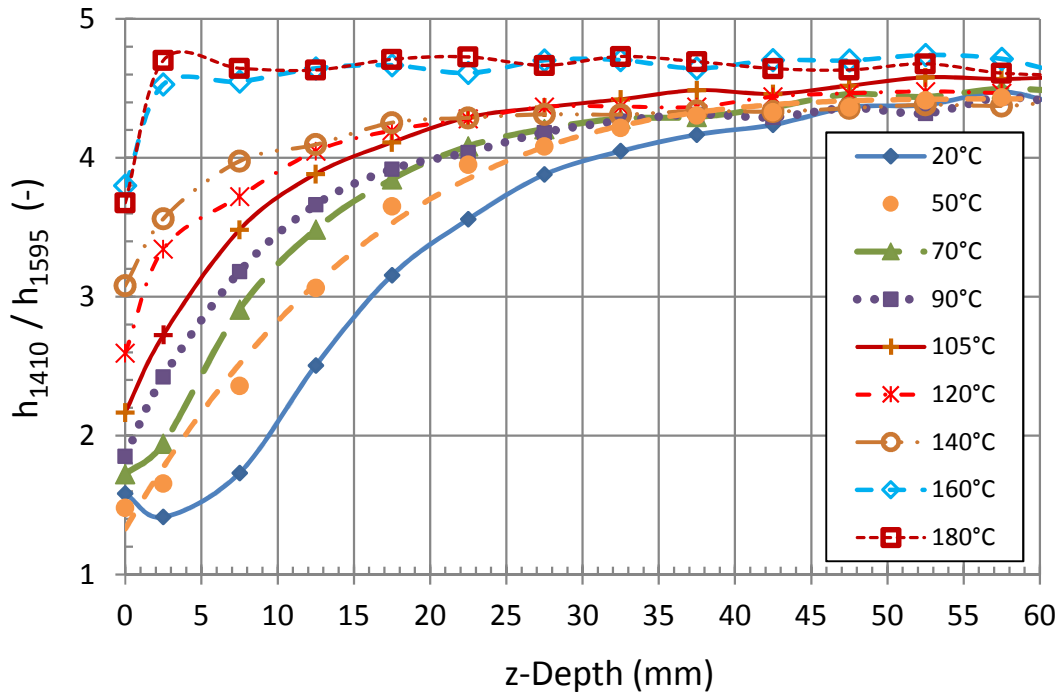


Figure 9: Evolution of the h_{1410}/h_{1595} (isocyanurate/phenyl) peak height ratio as a function of mold temperature for all PIR foam samples at $t \sim 4500$ h. The lines are only guides for the eyes.

In the case of PIR insulation foam boards, the double belt of the production line is usually operated within a temperature range of 65 to 80°C to ensure enough adhesion between the PIR foam and the facing. As a complement to our laboratory study on small samples, temperatures have been estimated directly on the production line of PIR foam insulation panels. For that purpose, self-adhesive thermometer strips (VWR Cat. No. 621-9103) have been placed under the facing at the level of the laydown table (just before the contact with the unexpanded reactive mixture) and maximum temperatures reached during foaming at the interface of the foam and the facing were typically comprised between 77 and 82°C in the majority of cases. Interestingly, the evolution of the isocyanurate/phenyl ratio as a function of depth for $T \sim 70^\circ\text{C}$ and reported in Figure 9 compares well with the results obtained for commercial products taken in the European market [25]. PIR/PUR gradients were also reported by Gahlen et al. [19] on commercial polyisocyanurate-based metal-foam composite elements (obtained from Covestro) of varying thickness (40, 60 and 100 mm). However,

these gradients were limited to the first 10-15 mm (instead of 20-30 mm in our case) on each face while the metal sheets were pre-heated to about 60°C. In addition, these authors observed a lower intensity of the isocyanurate signal for the lower cover layer with respect to the upper one. This phenomenon was attributed to the presence of an adhesion promoter applied to the lower cover sheet and/or to the difference of heat exchange of the foam with the lower metal sheet and the upper metal sheet. It should be noted that gradients in PIR/PUR ratio were also sometimes found along the width (cross machine direction) of PIR foam panels (Index around 250) near the lateral edges [21]. It appears from all these cases that the level of heating usually observed on production lines of PIR foam insulation panels is not high enough to prevent chemical gradients. However, Figure 9 clearly indicates that increasing T_{mold} allows to boost the surface isocyanurate content to a level almost identical to that present in the core and thus, it seems pointless to exceed 160°C. However, the sharp fall in isocyanurate/phenyl peak height ratio observed for $T_{\text{mold}} \geq 160^\circ\text{C}$ within the first 5 mm is striking because it was expected that the gradient would completely disappear for a mold temperature in the order of the maximum temperature reached in the center of the foam ($T_{\text{max}} \sim 160^\circ\text{C}$). This is clearly not the case and the discrepancy may be explained by a too short curing time (15 min in our case) with respect to the time spent at high temperatures in the core (where adiabatic conditions should take effect) and/or by the degradation of the polymer network at the surface of the mold (this point will be discussed in more detail in section 3.2.2).

Similarly, the vibration frequency (peak position) of isocyanurate peaks after 4500 h was systematically measured in the first 60 mm for the different mold temperatures and reported in Figure 10. At low mold temperature ($T \sim 20^\circ\text{C}$), the C-N (stretching vibration) frequency of isocyanurate ring varies from 1411cm^{-1} (surface) to around 1408cm^{-1} (core) which gives a frequency variation $\Delta\nu$ of around 3 cm^{-1} . However, this frequency shift almost disappears at high temperature with $\Delta\nu \sim 1\text{ cm}^{-1}$ for $T_{\text{mold}} \sim 180^\circ\text{C}$. As shown previously, all $\nu_{\text{C-N}} = f(z)$ curves converge towards an average value of about $1407.4 \pm 0.2\text{ cm}^{-1}$ (for $55 \leq z \leq 60\text{ mm}$) which confirms that the isocyanurate content is maximal in the core and is practically independent of T_{mold} .

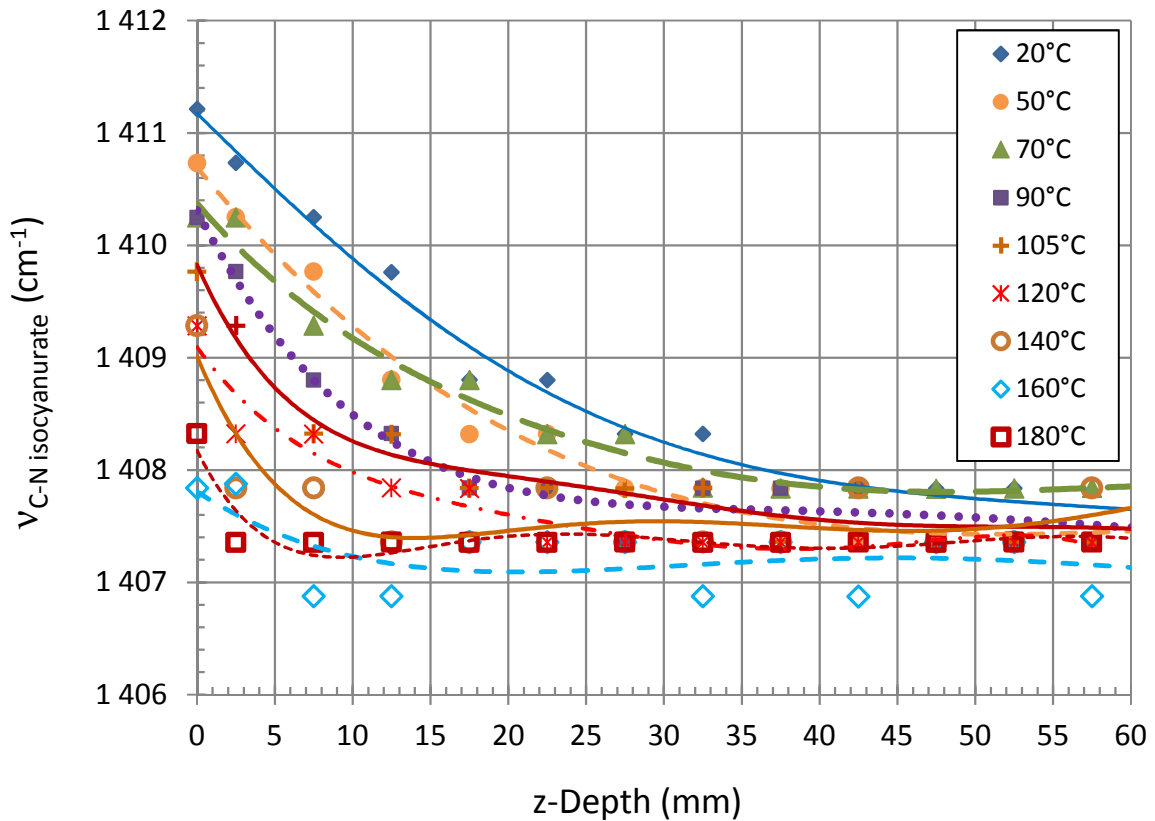


Figure 10: Evolution of the maximum intensity position of the C-N stretching vibration of isocyanurate ring as a function of surface temperature for all PIR foam samples at $t \sim 4500$ h. The lines are only guides for the eyes.

Based on the relationship between the C-N frequency of isocyanurate ring and the h_{1410}/h_{1595} peak height ratio reported in Figure 8, it then becomes interesting to compare Figures 9 and 10. This is done in Figure 11 where the data plotted clearly indicate that the peak maximum (frequency) of isocyanurate rings of the foam samples decreases linearly from 1411 to 1407 cm^{-1} (correlation coefficient of about 0.94) with the increase in the h_{1410}/h_{1595} peak height ratio from 1.4 to 4.8. Please note that the data volume was intentionally limited to values corresponding to depth varying between 0 and 40 mm (the region of gradients) so as not to overload the graphic (bottom right region). It is worth noting that similar frequency shifts have been found in the case of PIR foam insulation panels taken from the European market when probed at different depths [25].

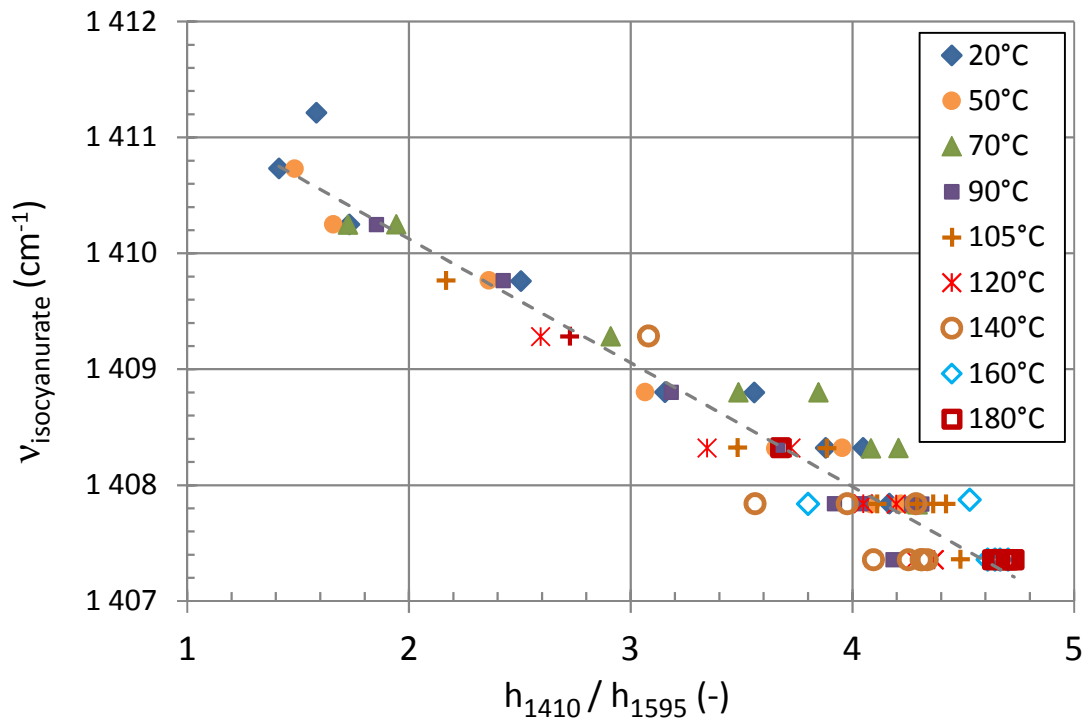


Figure 11: Evolution of C-N frequency of isocyanurate ring (peak maximum) as a function of isocyanurate/phenyl (h_{1410}/h_{1595}) height ratio for all PIR foam samples at $t \sim 4500$ h. The data volume was intentionally limited to values corresponding to depth varying between 0 and 40 mm so as not to overload the graphic. The dashed line corresponds to the best-fit line through all the data points with a linear regression ($R^2 \sim 0.94$).

Based on research findings [38,37,21,48], the isocyanurate gradients reported in Figures 9 and 10 would be attributed to the occurrence of heat loss at the surface of the foam which leads to temperature difference between the core and the surface of the foam, the highest temperature being at the center where the reaction should proceed more or less adiabatically. Indeed, the exothermic reactions that can occur during the polymerization process do not lead to the same temperature variation at the heart of the foam or on the surface just under the facing. For instance, temperature measurements were taken on a 100 mm thick PIR foam panel taken from a production line (right after the diagonal saw) and temperature difference of $\Delta T \sim 88^\circ\text{C}$ were estimated between the outer layer ($z \sim 10$ mm) and the core ($z \sim 60$ mm) [25]. More in-depth investigation about thermal gradients

occurring during the curing process of solid thermosets can be found in the literature. It is well accepted that the temperature variation at a specific location on the studied sample depends on the ratio of the heat dissipation rate to the heat generation rate [10]. Several authors [49,50] solved the differential equations describing the cure of a thermoset in a slab-shaped heated mold with a constant wall temperature (T_w) and demonstrated that the temperature profile and its evolution with time mostly depend on the critical parameter of the process defined as

$$\beta = AL^2/k \text{ (m}^3 \cdot \text{°C/J)} \quad (5)$$

where A (s^{-1}) is the Arrhenius pre-exponential factor or specific reaction rate, L (m) is the part thickness which is assumed to be much less than the other two dimensions and k (W/m.K) is the thermal conductivity of the polymer. For a thin sample and/or high thermal conductivity material, $\beta \rightarrow 0$ (heat diffuses much more rapidly than it is produced) and the maximum temperature reached during curing (T_{max}) is close to that of the wall (T_w) (quasi-isothermal conditions of curing). On the contrary, for a thick sample and/or low thermal conductivity material, $\beta \rightarrow \infty$ (the system behaves adiabatically) and $T_{max} \sim T_0 + \Delta T_{ad}$ where T_0 and ΔT_{ad} correspond to the initial temperature of the reactants and the adiabatic temperature rise, respectively. Between these two extreme values (i.e. for intermediate values of β), it was found that T_{max} can occur at intermediate position between the core and the wall and/or that T_{max} can rise beyond these two limits by the addition of heat generation and heat transferred from the wall. In our case, adiabatic conditions should prevail in the core of the PIR foam since foam samples are both thick and characterized by a low thermal conductivity ($\lambda \leq 30$ mW/m.K), which is in line with the data reported in Figure 9. In addition, Williams et al. [50] demonstrated that the maximum temperature (T_{max}) that may be attained in the cure of a thermoset in a mold with constant wall temperature may be higher than the sum of the wall temperature and the adiabatic temperature rise ($\Delta T_{max} > \Delta T_{ad} + T_w$) when the heat diffusion rate is equal or slightly higher than the heat production rate. If this were the case in our study, one could expect an increase in isocyanurate content in the core for the highest T_{mold} but there is no clear trend in the evolution of isocyanurate/phenyl ratio

(h_{1410}/h_{1595}) and/or isocyanurate peak maximum frequency (ν_{C-N}) as a function of T_{mold} in the core of the foam bun (layer 55-60 mm) (SI3). As a result, it can be asserted that the material located at the core of the foam undergoes a mostly adiabatic cure (i.e. it is not influenced by the wall temperature in a significant way) while the foam surface in contact with the heating element undergoes an almost isothermal curing temperature. The adiabatic conditions prevailing in the core of the foam should facilitate the formation of isocyanurate (higher conversion), leading to a kind of self-sustained trimerization reaction (trimerization of isocyanate is highly exothermic), as long as free isocyanates are available and mobile enough to be brought into contact. Given the inextricable linkage between isocyanurate content and temperature, it should be pointed out that the exothermicity generated by the cross-linking is stopped or at least strongly slowed down when the T_g of the PIR matrix reaches the temperature of the mold, because of the vitrification phenomenon. As a result, selecting a wall temperature lower than the maximum temperature at which the system can vitrify (T_g^∞) would prevent the material near the wall from reaching the maximum conversion. In those conditions, it is thus reasonable to say that temperature gradients occurring in the PIR foam panels along the depth (z-axis) led to isocyanurate gradients, but the question now is whether the increase of T_{mold} could lead to the increase in the mechanical properties of the foam base material and, more importantly, in the stiffness of the PIR foam under the facing.

3.2.2. Evolution of Shore hardness as a function of depth for the various mold temperatures ($t \sim 4500$ h)

All the above results unambiguously demonstrated that increasing the mold temperature increases the isocyanurate content up to a thickness of about 30 mm, but does this really have a positive impact on the rigidity of the foam surface, as one would expect? To verify this hypothesis, the evolution of Shore hardness (type H00, ASTM Standard D-2240) was systematically measured in the rise direction as a function of depth and reported in Figure 12 for each mold temperature. In addition, Figure 13 highlights the effect of mold temperature on Shore hardness by solely depicting the values measured

at the surface (under the facing) and in the core ($z \sim 47.5$ mm). Unambiguously, it is clearly demonstrated that the hardness at the surface drastically decreases from around 80 to 63 Shore OO as the mold temperature increases from 25 to 180°C. It is also seen in Figure 13 that the $H_{OO}=f(T_{mold})$ curve (surface) seems to be roughly linear up to $T_{mold} \sim 120^\circ\text{C}$ beyond which it starts to drop significantly. Deeper into the foam, all curves reported in Figure 12 converge towards a value of about 70 Shore OO (typically for $z \geq 30$ mm), which means that beyond this depth the Shore hardness seems to be independent of the mold temperature, as shown in Figure 13 for the core. It follows that the Shore hardness decreases as the depth increases for $T_{mold} \leq 120^\circ\text{C}$ while it increases for $T_{mold} \geq 180^\circ\text{C}$. The Shore hardness remains almost constant between those two mold temperatures.

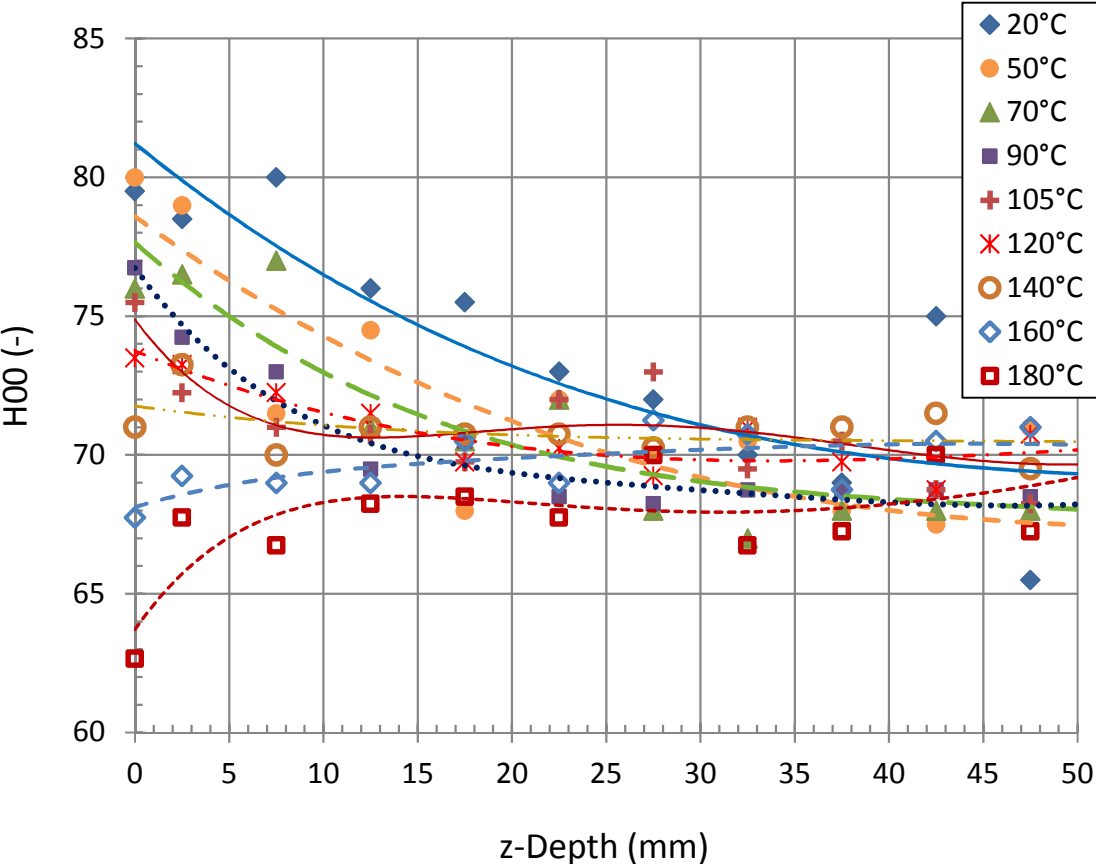


Figure 12: Evolution of the Shore hardness (type OO) as a function of depth for the different mold temperatures ($t \sim 4500$ h). The lines are only guides for the eyes.

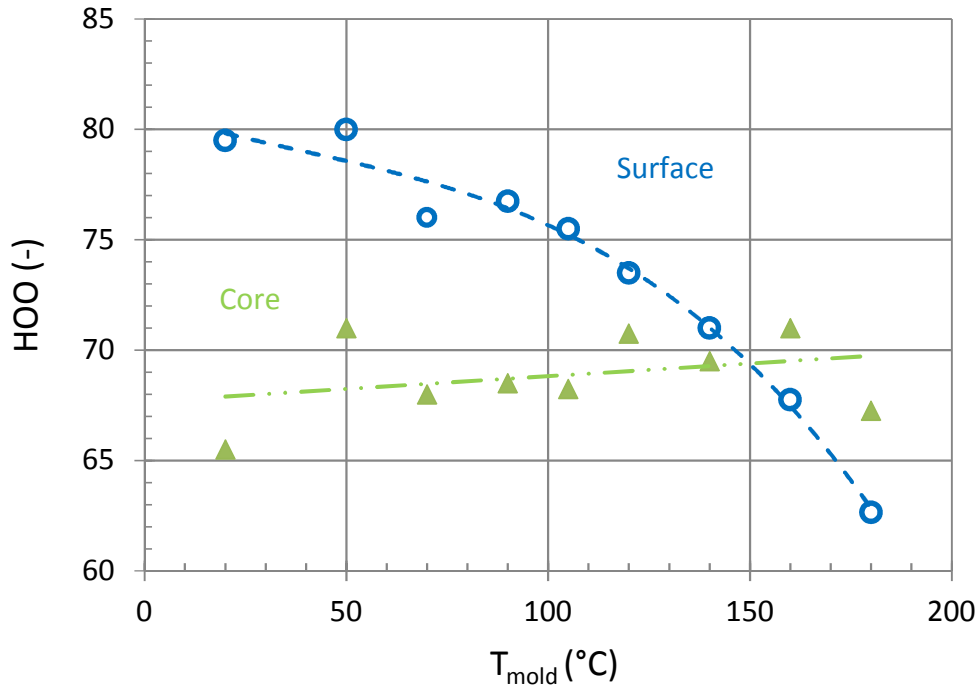


Figure 13: Evolution of the Shore hardness (type OO) at the surface ($z \sim 0$ mm) and in the core ($z \sim 47.5$ mm) as a function of mold temperature ($t \sim 4500$ h). The lines are only guides for the eyes.

Even if the Shore hardness of the foam is not determined solely by its elastic modulus, but also depends on the compressive strength and on the viscoelastic behavior of the foam (ASTM D2240-05), it is reasonable to say that the decrease in Shore hardness (at the surface) with the increase of T_{mold} means that the Young's modulus of the foam under the facing becomes smaller. This outcome is just the opposite of our expectations since it was hoped that the increase in isocyanurate content would increase the Young's modulus of the foam base material [19], thereby increasing the stiffness of the foam under the facing. However, this is not the only study that follows that direction. For instance, it was found for PIR foams made at almost constant density ($29.1 \leq \rho \leq 30.1 \text{ kg/m}^3$) that their compressive strength in the rise direction significantly decreases from 269 kPa to 196 kPa as the isocyanate index increases from 257 to 554 [51]. More often, the authors concluded that the NCO/OH ratio had no significant effect on the compressive strength as it was the case for PIR foams ($\rho \sim 33.1 \pm 0.4 \text{ kg/m}^3$) prepared at indexes varying between 105 and 1500 [52] or for water-blown PIR

foam ($\rho \sim 40 \text{ kg/m}^3$) prepared for metal-faced sandwich panels with isocyanate index varying between 175 and 300 [53]. In the end, the increase in isocyanurate content seems to have a positive effect on mechanical properties only in very few cases. Gilbert [54] demonstrated that the compressive strength (rise direction) of PIR foams increased from 143 kPa to 186 kPa ($\Delta\sigma \sim +30\%$) as the isocyanate index increased from 225 to 400, but these results may potentially be attenuated by the increasing density from 27.4 to 30.4 kg/m^3 .

An alternative possibility to explain the increase in Shore hardness of the PIR foam as mold temperature decreases may be related to the solid-state post-cure reaction mechanism occurring during aging at room temperature (see section 3.1.2 with the work of Prisacariu et al. [43]). In our case, the formation of new urea groups by reaction of residual -NCO with atmospheric humidity could potentially increase the stiffness of the foam base material. In addition, the data reported in Figure 7 indicates that the excess -NCO group consumption increases as the temperature decreases during aging and it is thus expected that the post-consolidation of the polymer network could be more pronounced at low mold temperatures. However, it is not possible to conclude at this stage because the evolution of Shore hardness at $t \sim 1 \text{ h}$ is unknown. Another possibility is the effect of physical aging ($T < T_g$) of the thermoset network occurring during post-cure. As already mentioned in the introduction, physical aging was found to reduce free volume (increase of density), increasing the energy of intermolecular interactions (Van der Waals forces) and the Young's modulus of the polymer network in the glassy state [10]. Nevertheless, it is the authors' belief that the expected variations in the mechanical properties of the foam base material would not be high enough to justify the huge differences of Shore hardness H00 values reported in Figure 10 at the surface ($z \sim 0 \text{ mm}$) and more work is needed on foam characterization to explain our results.

3.2.3. Evolution of the local foam density as a function of depth for the various mold temperatures (t~4500 h)

Another explanation for the decrease in surface Shore hardness (H00) with the increase in T_{mold} may be that the density and/or the morphology of the foam at the surface would have sufficiently changed to overcome the possible increase in the rigidity of the foam base material with the increase in mold temperature. Indeed, when talking about the factors that control foam mechanical properties, one of the most important is surely the void fraction as defined by

$$V_{foam}=1-(\rho_{foam}/\rho_{solid}) \quad (6)$$

where ρ_{foam} is the density of the foam and ρ_{solid} the density of the material constituting the cells [55]. Interestingly, many of the mechanical properties (P) of low relative density foams (typically, $\rho_{foam}/\rho_{solid}<0.4$) depend on the relative density according to a power law and can be described by the following equation

$$\frac{P_{foam}}{P_{solid}} = C \left(\frac{\rho_{foam}}{\rho_{solid}} \right)^n \quad (7)$$

where C and n are parameters which need to be experimentally determined for each foam system [55,56,57,58,59]. The exponent, n, depends on the temperature and typically ranges between 1 and 2 for the elastic modulus [57,60]. De Gisi et al. [57] compared the compressive properties of PUR foams in the temperature range -54°C to 163°C and reported a value of $n\sim 1.75$, while Goods et al. [61] obtained a value of $n\sim 1.6$ for the room temperature modulus of PUR foams. From a purely theoretical point of view, Gibson et al. [55] examined the variation of elastic modulus using a cubic cell model and demonstrated that the value of n depends on the relative proportion of material in the cell struts with respect to the wall (f_s) according to the following equation:

$$\frac{E_{foam}}{E_{solid}} \approx f_s^2 \left(\frac{\rho_{foam}}{\rho_{solid}} \right)^2 + (1 - f_s) \frac{\rho_{foam}}{\rho_{solid}} + \frac{p_0(1-2v_{foam})}{E_s(1-\rho_{foam}/\rho_{solid})} \quad (8)$$

where p_0 is the cell pressure. The second term in the right part of the equation corresponds to the membrane stresses associated with the presence of walls (closed cell) while the last term is the

contribution of gas pressure which can be neglected in the case of PUR/PIR foams ($T_{amb} < T_g$). For open cell foams ($f_s=1$), equation 8 reduces to equation 7 with $C=1$ and $n=2$. It is noteworthy that the effect of cell faces on stiffness should be relatively minor in the case of low-density PUR and PIR foams, because the strut thickness is relatively high with respect to the wall thickness [56]. The foam density curves, $\rho=f(z)$, obtained for the various T_{mold} are plotted as a function of z in Figure 14 while Figure 15 gathers the evolution of density as a function of T_{mold} for the surface (layer between $z=0$ mm and $z=5$ mm) and the core (layer between $z=45$ mm and $z=50$ mm), exclusively. It appears that the density at the surface (layer between $z=0$ and $z=5$ mm) falls from 45 kg/m^3 to about 30.5 kg/m^3 as the mold temperature increases from 25 to 180°C , respectively. On the contrary, the foam density can be considered as constant for $z \geq 30$ mm, meaning that the foam density decreases from the surface to the core and that this decrease tends to disappear as the mold temperature increases. A more detailed analysis of the foam density in the core (average value calculated for z varying between 30 and 100 mm) indicates, however, that there is a slight increase in the foam density from 28 to around 30.4 kg/m^3 as the mold temperature increases from 20 to 180°C (SI4). This may at first seem counter-intuitive, as one might assume that higher mold temperatures could slightly raise the core temperature (higher expansion pressure leading to lower density). However, it is likely that the higher mold temperature increases the amount of blowing agents evaporated near the bottom wall [62] and/or favors a faster crosslinking at the expense of higher expansion ratios, leading to a slight increase in the foam density at the core. In the end, the density variation ($\Delta\rho$) between the surface and the core can reach a value as high as 16 kg/m^3 for $T_{mold} \sim 20^\circ\text{C}$, as shown in Figure 16. It represents a maximum difference of around 50% with respect to the density of the core for $T_{mold} = 20^\circ\text{C}$. At the opposite end, the density variation becomes negligible ($\Delta\rho < 1 \text{ kg/m}^3$) for the highest temperatures ($T_{mold} \geq 160^\circ\text{C}$).

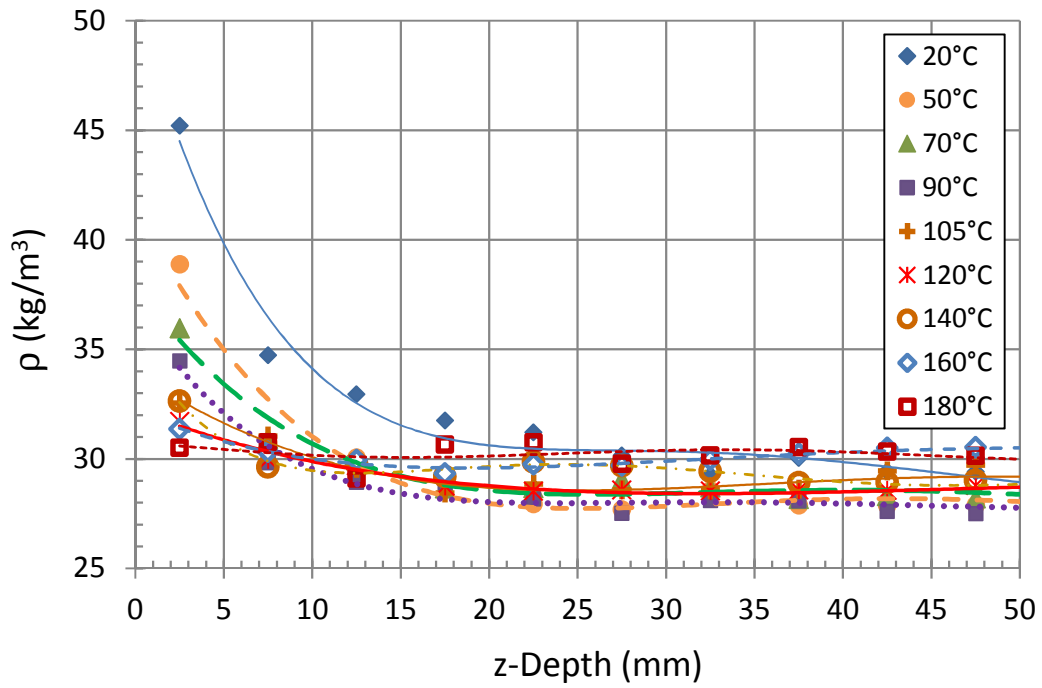


Figure 14: Evolution of the foam density as a function of depth for the different mold temperatures ($t \sim 4500$ h). The lines are only guides for the eyes.

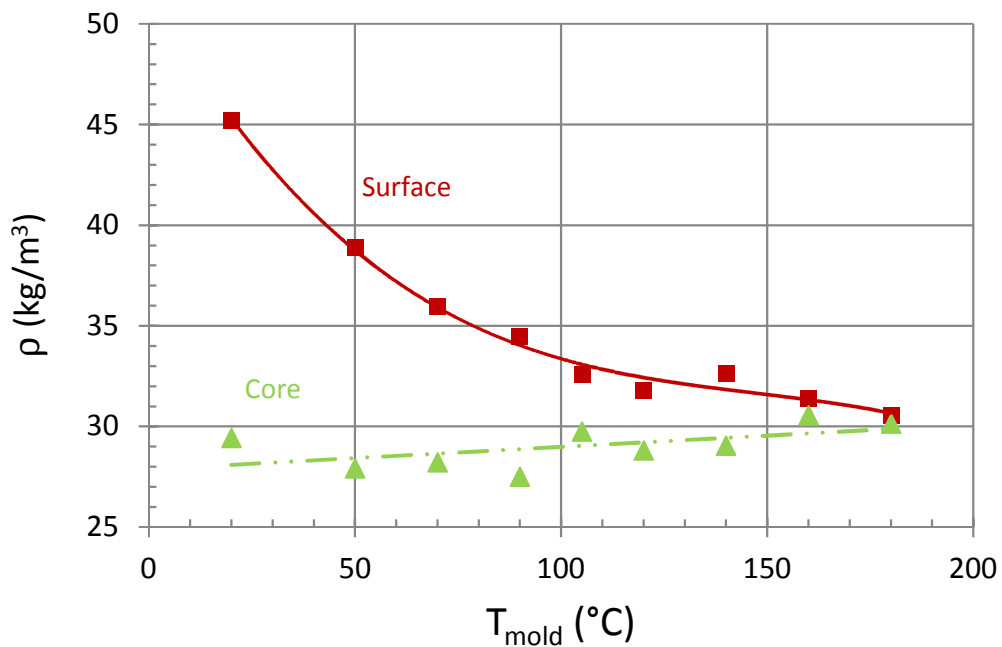


Figure 15: Evolution of foam density at the surface (layer between $z=0$ mm and $z=5$ mm) and in the core (layer between $z=45$ mm and $z=50$ mm) as a function of mold temperature ($t \sim 4500$ h). The lines are only guides for the eyes.

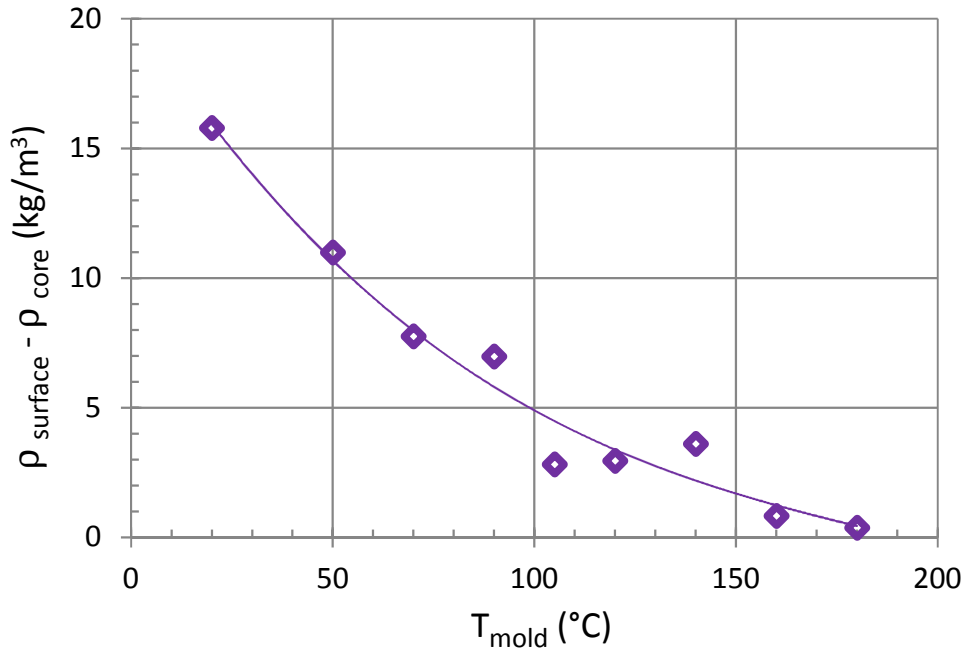


Figure 16: Effect of mold temperature on the difference between the surface (layer between 0 and 5 mm) and the core densities (layer between 45 and 50 mm). The line is only a guide for the eyes.

Several works have reported the presence of density gradients in various foaming systems, particularly in the case of molded foam [62,63,64,65]. Broadly speaking, density gradients in PUR/PIR foams are mainly attributed to the occurrence of heat loss at the surface of the foam. On the contrary, the low thermal conductivity and low thermal diffusivity of the foam [66] allows chemical reactions to occur under adiabatic conditions at the core of the foam. This major difference leads to a temperature difference during manufacturing between the core and the surface of the foam. In our case, temperature difference of $\Delta T_{\text{max}} \sim 75^\circ\text{C}$, 52°C and 27°C were found between $z=5$ mm and $z=60$ mm for $T_{\text{mold}} \sim 22^\circ\text{C}$, 70°C and 120°C , respectively (SI5). Similarly, we have reported in a previous study a temperature difference of about 88°C between $z=5$ mm and $z=60$ mm for a realistic 100 mm-thick PIR foam panel [25]. The higher temperature prevailing at the core of the foam will generate more gas pressure in each cell (because of the ideal gas law). This higher pressure in the cells will push the opposite walls of each cell apart, therefore increasing cell expansion and lowering the foam density of the core with respect to the surface. The higher the difference in T_{max} , the higher the difference in ρ_{foam} .

This phenomenon has been extensively studied in the case of integral skin foams used as structural materials for which the sides of the wall are voluntarily maintained at low temperature to create a material with a low-density foamed core surrounded by a nearly solid skin. An example of this type of polyurethane foams (overall density, $\rho \sim 485 \text{ kg/m}^3$) was prepared in a flat plate mold with wall temperature set at about 34°C . They were characterized by a core density as low as 230 kg/m^3 while the skin density reached values as high as 760 kg/m^3 [62]. To circumvent the issues associated with density gradients, Harbron et al. [63] proposed to increase the mold temperature in order to get more homogeneous water blown PUR foams. In that respect, the density variation ($\Delta\rho = \rho_{\max} - \rho_{\min}$ for a given mold temperature) was found to drop from $\Delta\rho \sim 124 \text{ kg/m}^3$ down to $\Delta\rho \sim 15 \text{ kg/m}^3$ as the mold temperature increased from 20 to 50°C (for an overall density $\rho \sim 800 \text{ kg/m}^3$).

In our work, the decrease in the foam density reported at the surface (layer between $z=0$ and $z=5\text{mm}$) with the increase of T_{mold} is in line with the data reported in the literature. It could be interesting to compare the effect of the increase in the polymer matrix modulus from the surface ($T_{\text{surface}} \sim 60^\circ\text{C}$) to the core ($T_{\text{core}} \sim 150^\circ\text{C}$) obtained from Gahlen et al. [19] with the effect of the decrease in the foam density (surface layer) observed in our case for $T_{\text{mold}} = 60^\circ\text{C}$ and 150°C . Making the hypothesis that the variation of the density of the foam base material (E_{solid}) with T_{mold} is negligible ($\Delta\rho_{\text{solid}}$ variations should be below 1%), it can be written from equation 7 that

$$\frac{E_{\text{foam}}^{T_1}}{E_{\text{foam}}^{T_2}} = \frac{E_{\text{solid}}^{T_1}}{E_{\text{solid}}^{T_2}} \left(\frac{\rho_{\text{foam}}^{T_1}}{\rho_{\text{foam}}^{T_2}} \right)^n \quad (9)$$

Taking a conventional value for the exponent $n=1.75$ and choosing $T_1=60^\circ\text{C}$ and $T_2=150^\circ\text{C}$, it ensues from Figure 15 ("surface" curve) that $\rho_{\text{foam}}^{60^\circ\text{C}}=37.5 \text{ kg/m}^3$ and $\rho_{\text{foam}}^{150^\circ\text{C}}=31.5 \text{ kg/m}^3$. The values $E_{\text{solid}}^{60^\circ\text{C}}=3.41 \text{ GPa}$ and $E_{\text{solid}}^{150^\circ\text{C}}=3.93 \text{ GPa}$ are gathered from the data of Gahlen et al. [19]. One then obtains the foam modulus ratio $E_{\text{foam}}^{60^\circ\text{C}}/E_{\text{foam}}^{150^\circ\text{C}} \sim 1.2$ which indicates that the elastic modulus of the foam prepared at low temperature should be higher (by about 20%) than that obtained at high temperature. This implies that the effect of foam density variation on the elastic modulus of the foam

should be more significant than the effect of the variation of E_{solid} (foam base material). This phenomenon is essentially driven by the exponent $n>1$ on the density reported in equation 7, which tends to enhance the influence of ρ_{foam} over that of the E_{solid} ($E_{foam} \propto E_{solid}(\rho_{foam})^{1.75}$). Let us return to the main objective of this work, namely preventing the formation of surface wrinkles. Based on equation 1, it can be written that

$$\frac{\varepsilon_c^{T_1}}{\varepsilon_c^{T_2}} \propto \left[\left(\frac{E_{substrate}^{T_1}}{E_{substrate}^{T_2}} \right) \left(\frac{E_{film}^{T_2}}{E_{film}^{T_1}} \right) \right]^{2/3} \quad (10)$$

Making the hypothesis that $T_2 > T_1$, it has been inferred in our case that $\left(\frac{E_{substrate}^{T_1}}{E_{substrate}^{T_2}} \right) > 1$. The facing used in the production of PIR foam panels is a multilayer laminate mainly composed of Kraft paper and thermoplastic polymers (such as PE, PP and PET) whose mechanical properties are temperature-dependent. As a result, the mechanical properties of the facing tend to decrease with increasing temperature which gives $\left(\frac{E_{film}^{T_2}}{E_{film}^{T_1}} \right) < 1$ and it is hard to conclude whether the quantity $\frac{\varepsilon_c^{T_1}}{\varepsilon_c^{T_2}}$ (see eq.10) will be greater or lower than unity. In addition to that, even if the critical strain is postponed at higher values when the temperature increases ($\varepsilon_c^{T_2} > \varepsilon_c^{T_1}$), this does not necessarily mean that the wrinkles will not appear because the compressive strain level (shrinkage) also depends on the mechanical resistance of the facing: the lower the mechanical resistance of the facing, the higher the compressive strain. However, the temperature of the facing should rapidly decrease during the post-cure treatment at room temperature (in particular for the highest temperatures) which should limit its influence on the shrinkage level. But the fact that the rigidity of the foam substrate decreases with the increase of mold temperature is not going in the right direction and should not prevent the formation of surface wrinkles.

Getting back to the Shore hardness, it therefore appears that it is not controlled by the isocyanurate content but is closely connected to the local (surface) foam density. The Shore hardness values

measured within the first 30 mm plotted in Figure 17 as a function of foam density seem to confirm that hypothesis, although there is some scatter in the data: the higher the foam density, the higher the Shore hardness. Nevertheless, it does not explain why the Shore hardness of the samples with $T_{\text{mold}} \geq 160^\circ\text{C}$ is lower at the surface than in the core while the corresponding densities of the surface layer and the core are almost the same. Some thermal degradation of the polymer matrix may potentially explain this decrease in surface Shore hardness at high temperatures. According to Montserrat [26] who studied the effect of isothermal curing of epoxy resins, devitrification of the thermoset can occur when the isothermal curing temperature is too high and may lead to the decrease of the crosslink density. In our case, it is well known that isocyanurate groups are thermally more stable than urethane groups, because of the absence of labile hydrogens in the isocyanurate ring [48]. Isocyanurate linkages dissociate at a temperature of about 350°C as opposed to 200°C for urethane linkages based on aryl-NCO/alkyl-OH [67,68,69]. In our study, the detailed analysis of IR spectra did not show any evidence of a significant drop of urethane content as shown by the constancy of urethane/isocyanurate ratio at $T_{\text{mold}} \geq 160^\circ\text{C}$ (Figure 6). Eventually, it is worth noting that the foam surface (after facing removal) carries brown stains which darken as the mold temperature increases. The characteristic shape of these stains suggests that they correspond to the area of the first contact of the liquid mixture (before any reactions) with the bottom face of the hot mold. It is the authors' belief that the liquid mixture could be "scorched" at the time it is poured into the hot mold, causing a significant decrease in the Shore hardness for $T_{\text{mold}} \geq 160^\circ\text{C}$. It should be emphasized that the core of the foam does not seem to be affected by this phenomenon while the maximum temperature can reach about 160°C . One possible explanation may be that the matrix is partly cross-linked and thus should be more able to withstand high temperatures. Another possible explanation could be related to the oxidation of the liquid mixture when it comes in contact with the bottom face of the mold while no oxygen molecules are available in the core of the foam. In any case, this phenomenon may also explain why the isocyanurate level (as probed by the h_{1410}/h_{1595} peak height ratio) is lower at the surface for $T_{\text{mold}} \geq 160^\circ\text{C}$ (see section 3.2.1).

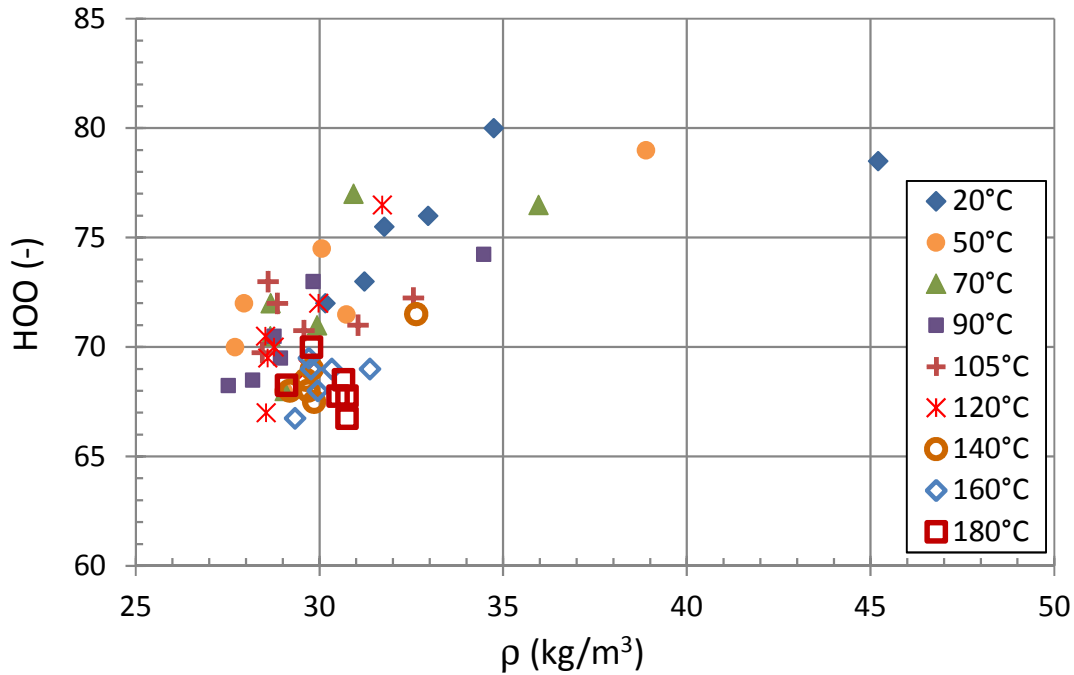


Figure 17: Evolution of Shore hardness as a function of foam density (ρ). The data volume was intentionally limited to values corresponding to depth varying between 0 and 30 mm so as not to overload the graphic.

3.2.4. Evolution of foam morphology as a function of depth for $T_{\text{mold}} \sim 25^\circ\text{C}$ ($t \sim 4500$ h)

One last question concerns the potential changes in the morphology of the cellular structure. Any variation in foam density is usually accompanied by a change of the size and the shape factor of cells. As a rule, the cells of PUR and PIR foams prepared in open mold tend to be elongated in the foam rise direction. Several authors [56,70,71] demonstrated for PUR foams that both the size and the geometrical anisotropy of cells decreased (less elongated in the rise direction) with increasing density. In our case, cell characteristics were investigated for the lower mold temperature ($T_{\text{mold}} \sim 25^\circ\text{C}$) in order to maximize the chance of seeing any difference in foam morphology between the surface (low temperature) and the core (high temperature). Despite a few discrepancies, Figure 18 indicates that both the average cell size (projected area diameter, d_A) and Feret aspect ratio (shape factor) increase with depth up to about 30 mm. With an average value $\theta \sim 90.5 \pm 2.5^\circ$ for the different layers ($\theta_{\text{max}} \sim 97^\circ$

and $\theta_{\min} \sim 85^\circ$), the average orientation angle (Feret angle) confirms that cells are mainly oriented vertically (rise direction) and that the difference in Shore hardness cannot be attributed to a variation of cell orientation. In addition, the relative constancy of cell population density ($\beta \sim (5.76 \pm 0.25) \times 10^6 \text{ cell/cm}^3$) over the whole block thickness tends to indicate that the level of coarsening (coalescence and/or Ostwald ripening) is similar across the whole block, despite the difference in temperature between the surface and the core. Similarly, Hatchett et al. [72] indicated in the case of molded PU foams that the cell dimensions increased from the side to the center of the foam processed at 25°C. The differences in size and aspect ratio of the cells may be explained by the higher temperature in the core which generates more gas pressure, channeled in the rise direction because lateral expansion is precluded. In addition to that, it has been demonstrated for PUR foams ($65 \text{ kg/m}^3 < \rho < 70 \text{ kg/m}^3$) of various molar mass per branching unit ($300 \text{ g/mol} < M_c < 1150 \text{ g/mol}$) that the cell elongation in the rise direction decreased with increasing M_c [31]. More precisely, the PUR foams with $300 \text{ g/mol} < M_c < 600 \text{ g/mol}$ were characterized by a cell aspect ratio in the range 1.2-1.4 but R decreased in the range 0.9-1.2 for $650 \text{ g/mol} < M_c < 1150 \text{ g/mol}$. One may ask whether the decrease of M_c of our PIR foams, as expected from the increase in isocyanurate content (crosslinking nodes) when moving from the surface to the core, may also favor the cell anisotropy. However, this is just an informed guess because it is not possible to separate these two causes. Whatever the case, Smits [73] theoretically argued that cell size can affect the mechanical properties of a foam, all other things being equal. In practice, changing the cell size without affecting other characteristics such as foam density and/or cell shape factor is not straightforward and to the best of our knowledge there is no real rules linking the cell size and mechanical properties such as compression modulus and/or stress at yield. In contrast, it has been demonstrated that increasing cell aspect ratio should both increase the elastic modulus and stress at yield loaded in the rise direction [56,74]. According to Hawkins et al. [75], it is one of the primary reasons why the compressive modulus and collapse stress depend on the vertical positions for PUR foams made in tall mold while the density variations are smaller than 4%. In our case, the increase in cell aspect ratio should slightly compensate the decrease in foam density in

the core but seemingly not enough, judging from the decrease in Shore hardness ($T_{\text{mold}} \sim 20^\circ\text{C}$) as one moves from the surface to the core (Figure 12).

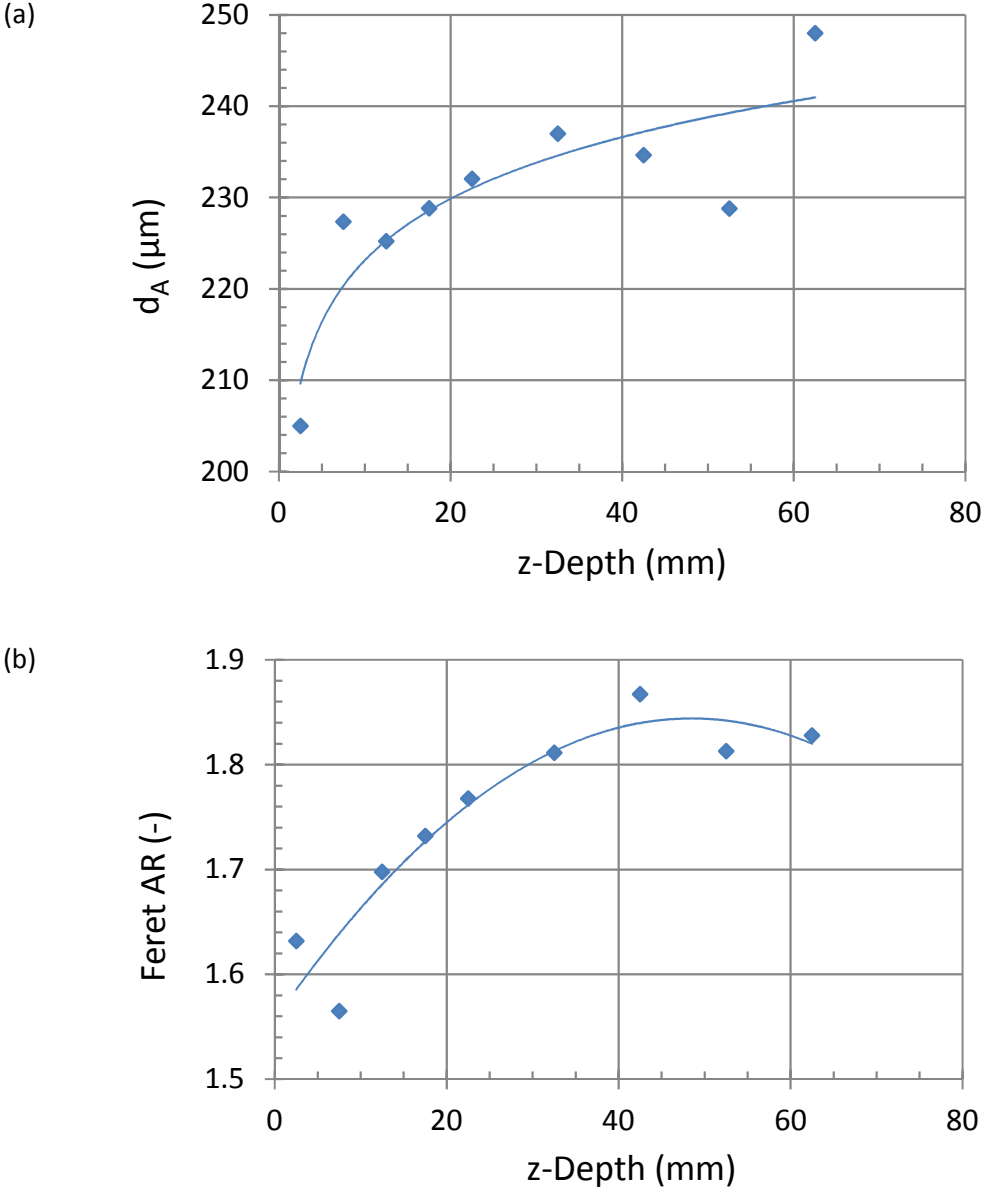


Figure 18: Evolution of (a) Projected area diameter and (b) Feret Aspect Ratio as a function of depth (z axis) for the $T_{\text{mold}}=25^\circ\text{C}$ ($t \sim 4500$ h). The lines are only guides for the eyes.

4. Conclusions

The main purpose of this work was to determine whether the increase in the double-belt temperature (as simulated by the mold temperature in our case) would allow an increase in the rigidity of the foam surface, with the aim of restraining or even preventing the formation of two-dimensional wrinkles of PIR foam insulation panels. For that purpose, model PIR foam samples were prepared at different mold temperatures and were chemically analyzed using ATR-FTIR spectroscopy while a Shore durometer (type OO) was used to estimate the foam rigidity. Both analyses were performed at different depths from the surface to the core of the material, and the corresponding local densities were also determined.

The isocyanurate content of the foam surface (under the facing) was found to increase with the increase in mold temperature. In addition, profiles of isocyanurate content (in the rise direction) indicate that the strong chemical gradients occurring in the first 20-30 mm for a non- or weakly heated mold tend to disappear as the mold temperature increases. These chemical gradients are directly related to the thermal gradient occurring during manufacturing, because heat loss is strongly minimized in the core (adiabatic curing) of the foam bun thanks to the intrinsic thermal insulation properties of the foam.

The foam rigidity at the surface was found to strongly depend on the mold temperature but somewhat surprisingly, the surface Shore hardness (type OO) was found to decrease with the increase of mold temperature. This result was explained by the decrease of foam density at the surface as the mold temperature increases (the foam density at the core can be considered as independent of T_{mold} in first approximation). Contrary to some expectations, increasing the temperature of the production line (top and bottom surface of the double-belt) should therefore not allow to increase the rigidity of the foam surface (under the facing) and, consequently, should not constrain the formation of two-dimensional wrinkles in high thickness PIR foam boards. Nevertheless, this result does not exclude the possible increase in the elastic modulus and/or stress at yield of the foam base material with the surface

temperature (in relation with a higher isocyanurate content) but the effect is, apparently, not strong enough to compensate for the decrease of foam local density (under the facing). Perhaps one solution might be to enhance the formation of isocyanurate after the establishment of the foam structure (to keep foam density the same), which potentially could be done by increasing the aging temperature while keeping T_{mold} as low as possible to maintain a higher local foam density.

5. Data availability

The raw/processed data required to reproduce these findings cannot be shared at this time due to legal or ethical reasons.

Acknowledgements

The authors are grateful to Vincent Barraud and Alexandre Fougeron (R&D SOPREMA, Saint-Julien-du-Sault) for fruitful discussions. The authors wish to thank William René for online temperature measurements (R&D SOPREMA, Saint-Julien-du-Sault). This project was made possible with the financial support of SOPREMA.

References

- [1] Bowden N., Brittain S., Evans A.G., Hutchinson J.W., Whitesides G.M. "Spontaneous Formation of Ordered Structures in Thin Films of Metals Supported on an Elastomeric Polymer", *Nature* 1998, Vol.393, pp.146-149
- [2] Reignier J., Sarbu A., Barraud V. "Spontaneous formation of two-dimensional wrinkles in poly(urethane-isocyanurate) rigid foam boards" *Journal of Cellular Plastics* 2020, Vol.56 (N°3), pp.297-315.
- [3] Modesti M., Lorenzetti A. "An Experimental Method for Evaluating Isocyanurate Conversion and Trimer Formation in Polyisocyanurate-Polyurethane Foams" *European Polymer Journal* 2001, Vol.37, pp.949-954

- [4] Hilado C.J. "Friability Tests for Rigid Cellular Plastics" *Journal of Cellular Plastics* 1969, Vol.5, pp.56-60
- [5] Kaiser T. "Highly Crosslinked Polymers" *Progress in Polymer Science* 1989, Vol.14, pp.373-450
- [6] Askadskii A.A., Goleneva L.M., Bychko K.A., Afonicheva O.V. "Synthesis and Mechanical Behavior of Functionally Gradient Polyisocyanurate Materials Based on Hydroxy-Terminated Butadiene Rubber" *Polymer Science, Ser.A* 2008, Vol.50, pp.781-791
- [7] Bell J.P. "Mechanical Properties of a Glassy Epoxide Polymer: Effect of Molecular Weight Between Crosslinks" *Journal of Applied Polymer Science* 1970, Vol.14, pp.1901-1906
- [8] Shimbo M., Nishitani N., Takahama T. "Mechanical Properties of Acid-Cured Epoxide Resins with Different Network Structures" *Journal of Applied Polymer Science* 1984, Vol.29, pp.1709-1721
- [9] Lesser A.J., Kody R.S. "A Generalized Model for the Yield Behavior of Epoxy Networks in Multiaxial Stress States" *Journal of Polymer Science Part B: Polymer Physics* 1997, Vol.35, pp.1611-1619
- [10] Pascault J.P., Sautereau H., Verdu J., Williams R.J.J. "Thermosetting Polymers" Dekker, pp.477, 2002
- [11] Crawford E., Lesser A.J. "The Effect of Network Architecture on the Thermal and Mechanical Behavior of Epoxy Resins" *Journal of Polymer Science Part B: Polymer Physics* 1998, Vol.36, pp.1371-1382
- [12] Long T.R., Elder R.M., Bain E.D., Masser K.A., Sirk T.W., Yu J.H., Knorr Jr D.B., Lenhart J.L. "Influence of molecular weight between crosslinks on the mechanical properties of polymers formed via ring-opening metathesis" *Soft Matter* 2018, Vol.14, pp.3344-3360
- [13] Rackley F.A., Turner H.S., Wall W.F. "Preparation of Crosslinked Polymers with Increased Modulus by High-Pressure Polymerization" *Journal of Polymer Science: Polymer Physics* 1974, Vol.12, pp.1355-1370
- [14] Haward R., Young R.J., "The Physics of Glassy Polymers" 1997 Chapman & Hall
- [15] Detwiler A.T., Lesser A.J. "Aspects of Network Formation in Glassy Thermosets" *Journal of Applied Polymer Science* 2010, Vol.117, pp.1021-1034
- [16] Enns J.B, Gillham J.K. "Effect of the Extent of Cure on the Modulus, Glass Transition, Water Absorption, and Density of an Amine-Cured Epoxy" *Journal of Applied Polymer Science* 1983, Vol.28, pp.2831-2846
- [17] Bellenger V., Dhaoui W., Morel E., Verdu J. "Packing Density of the Amine-Crosslinked Stoichiometric Epoxy Networks" *Journal of Applied Polymer Science* 1988, Vol.35, pp.563-571
- [18] Askadskii A.A., Goleneva L.M., Afanas'ev E.S., Petunova M.D. "Gradient Polymeric Materials" *Review Journal of Chemistry* 2012, Vol.2, (2), pp.105-152

- [19] Gahlen P., Fröbel S., Karbach A., Gabriel D., Stommel M. "Experimental Multi-Scale Approach to Determine the Local Mechanical Properties of Foam base Material in Polyisocyanurate Metal Panels" *Polymer Testing* 2021, Vol.93, 106965
- [20] De Haset J.A., Andrews J.E., McClusky J.V., Priester Jr R.D., Harthcock M.A., Davis B.L. "Characterization of Polyurethane Foams by Mid-Infrared Fiber/FT-IR Spectrometry" *Applied Spectroscopy* 1993, Vol.47, pp.173-179
- [21] Burns S.B., Schmidt E.L. "The PIR/PUR ratio: A Novel Trimer Conversion Test with High Correlation to the Factory Mutual Calorimeter for HCFC-141b Blown Polyisocyanurate Foams" *Journal of Cellular Plastics* 1995, Vol.31, N°2, pp.137-153
- [22] Priester Jr R.D., Mc Clusky J.V., O'Neill R.E., Turner R.B., Harthcock M.A., Davis B.L. "FT-IR- A Probe into the Reaction Kinetics and Morphology Development of Urethane Foams" *Journal of Cellular Plastics* 1990, Vol.26, pp.346-367
- [23] Raffel B., Loevenich C.J. "High Throughput Screening of Rigid Polyisocyanurate Foam Formulations: Quantitative Characterization of Isocyanurate Yield via the Adiabatic Temperature Method" *Journal of Cellular Plastics* 2006, Vol.42, pp.17-47
- [24] Bhattacharjee D., Engineer R. "An Improved Technique for the Determination of Isocyanurate and Isocyanate Conversion by Photoacoustic FTIR" *Journal of Cellular Plastics* 1996, Vol.32, pp.260-273
- [25] Reignier J., Méchin F., Sarbu A. "Chemical gradients in PIR foams as probed by ATR-FTIR analysis and consequences on fire resistance" *Polymer Testing* 2021, Vol.93, 106972
- [26] Montserrat S. "Vitrification and Further Structural Relaxation in the Isothermal Curing of an Epoxy Resin" *Journal of Applied Polymer Science* 1992, Vol.44, pp.545-554
- [27] Halary J.L. "Structure-Property Relationships in Epoxy-Amine Networks of Well-Controlled Architecture" *High Performance Polymers* 2000, Vol.12, pp.141-153
- [28] Pascault J.P., Williams R.J.J. "Glass Transition Temperature Versus Conversion Relationships for Thermosetting Polymers" *Journal of Polymer Science: Part B: Polymer Physics* 1990, Vol.28, pp.85-95
- [29] Hale A., Macosko C.W. "Glass Transition Temperature as a function of Conversion in Thermosetting Polymers", *Macromolecules* 1991, Vol.24, pp.2610-2621
- [30] Carleton P.S., Proctor G.C. "Cure Conditions for Isocyanurate Polymers" *Journal of Elastomers and Plastics* 1989, Vol.21, pp.197-211
- [31] Stirna U., Beverte I., Yakushin V., Cabulis U. "Mechanical Properties of Rigid Polyurethane Foams at Room and Cryogenic Temperatures" *Journal of Cellular Plastics* 2011, Vol.47, pp.337-355
- [32] Duff D.W., Maciel G.E. "Monitoring Postcure Reaction Chemistry of Residual Isocyanate in 4,4'-Methylenebis(phenyl isocyanate) Based Isocyanurate Resins by ¹⁵N and ¹³C CP/MAS NMR" *Macromolecules* 1991, Vol.24, pp.387-397
- [33] Lee A., McKenna G.B. "Effect of Crosslink Density on Physical Ageing of Epoxy networks" *Polymer* 1988, Vol.29, pp.1812-1817

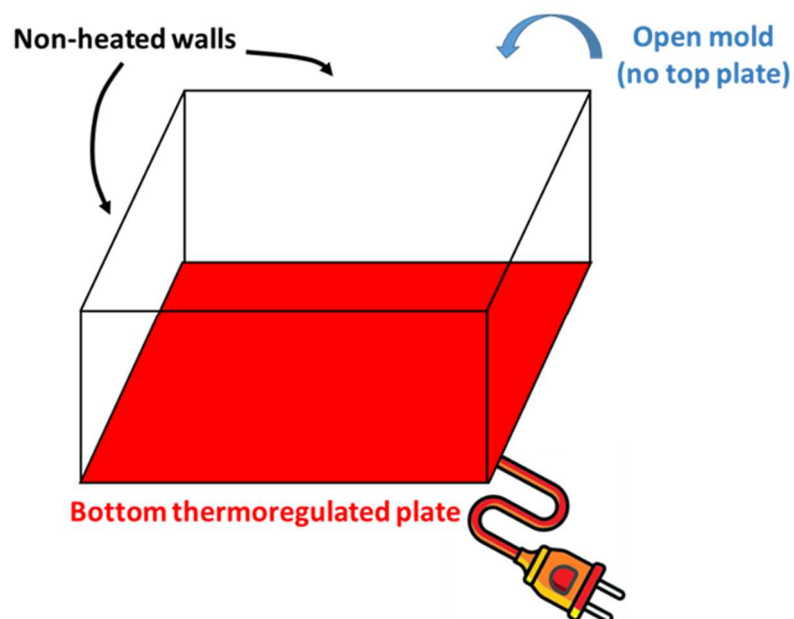
- [34] McGonigle E.-A., Cowie J.M., Arrighi V. "Enthalpy Relaxation and Free Volume Changes in Aged Styrene Copolymers Containing a Hydrogen Bonding Co-Monomer" *Journal of Materials and Science* 2005, Vol.40, pp.1869-1881
- [35] Yoshida H., Kanbara H., Takemura N., Kobayashi Y. "Effect of Hydrogen Bond Formation on Physical Aging of Ethylene-Vinyl Alcohol Copolymers with Annealing Below T_g " *Sen-I Gakkaishi* 1983, Vol.39 (12), pp.50-56
- [36] Yoshida H., Nakamura K., Kobayashi Y. "Differential Scanning Calorimetric Study of Enthalpy Relaxation in Polystyrene, Poly(4-hydroxystyrene), and Their Copolymers" *Polymer Journal* 1982, Vol.14 (11), pp.885-859
- [37] Lövenich C.J., Raffel B. "A Quantitative Investigation of the Effect of the Recipe on the Trimer-yield in Polyisocyanurate Foams" *Journal of Cellular Plastics* 2006, Vol.42, pp.289-305
- [38] Mitchener G. "PIR technology: Developments and Solutions for a Demanding Industry" *Urethanes Technology International* 2012, Vol.29, pp. 34-37
- [39] Park D.H., Park G.P., Kim S.H., Kim W.N. "Effects of Isocyanate Index and Environmentally-Friendly Blowing Agents on the Morphological, Mechanical, and Thermal Insulating Properties of Polyisocyanurate-Polyurethane Foams" *Macromolecular Research* 2013, Vol.21, pp.852-859
- [40] Hoffman D.K. "Model System for a Urethane-Modified Isocyanurate Foam" *Journal of Cellular Plastics* 1984, Vol.20, pp.129-137
- [41] Špirková M., Kubin M., Dusek K "Side Reactions in the Formation of Polyurethanes: Model Reactions Between Phenylisocyanate and 1-Butanol" *Journal of macromolecular Science: Part A – Chemistry: Pure and Applied Chemistry*, Vol.24 (Issue 10), pp.1151-1166
- [42] Al Nabulsi A., Cozzula D., Hagen T., Leitner W., Müller T.E. "Isocyanurate formation during rigid polyurethane foam assembly: a mechanistic study based on *in situ* IR and NMR spectroscopy" *Polymer Chemistry* 2018, Vol.9, pp.4891-4899
- [43] Prisacariu C., Agherghinei I. "Reactions in solid state within polyurethanes. Kinetics and postcure reaction mechanism in casting polyurethane elastomers" *J.M.S. Pure Appl. Chem.* 2000, Vol.37, pp.785-806
- [44] Šebenik A., Osredkar U., Vizovišek I. "Identification of Oligomers in the Reaction of Polyols with Isocyanates by ^{13}C -NMR and GPC" *Journal of Macromolecular Science: Part A – Chemistry* 1986, Vol.23 (Issue 3), pp.369-379
- [45] Ionescu M. "Chemistry and Technology of Polyols for Polyurethanes" Vol.1, 2005, Rapra Technology Limited
- [46] Heintz A.M., Duffy D.J., Hsu S.L., Suen W., Chu W., Paul C.W. "Effects of Reaction Temperature on the Formation of Polyurethane Prepolymer Structures" *Macromolecules* 2003, Vol.36, pp.2695-2704
- [47] Kogon I.C. "Chemistry of Aryl Isocyanates. The Influence of Metal Carboxylates on the Aryl Isocyanate-Ethyl Carbanilate Reaction" *The Journal of Organic Chemistry* 1961, Vol.26 (Issue 8), pp.3004-3005

- [48] Reymore H.E. JR, Carleton P.S., Kolakowski R.A., Sayigh A.A.R. "Isocyanurate Foams: Chemistry, Properties and Processing" *Journal of Cellular Plastics* 1975, Vol.11, pp.328-344
- [49] Adabbo H.E., Rojas A.J., Williams R.J.J. "Critical Parameters for Thermoset Curing in Heated Molds" *Polymer Engineering and Science* 1979, Vol.19, pp.835-840
- [50] Williams R.J.J., Rojas A.J., Marciano J.H., Ruzzo M.M., Hack H.G. "General Trends in the Curing of Thermosets in Heated Molds" *Polymer-Plastics Technology and Engineering* 1985, Vol.24, pp.243-266
- [51] Imai Y., Inukai T. "Studies on General Properties of Urethane-Modified Polyisocyanurate Foams" *Journal of Cellular Plastics* 1983, Vol.19, pp.312-317
- [52] Nawata T., Kresta J.E., Frisch K.C. "Comparative Studies of Isocyanurate and Isocyanurate-Urethane Foams" *Journal of Cellular Plastics* 1975, Vol.11, pp.267-278
- [53] Naruse A., Nanno H., Inohara H., Fukami T. "Development of All Water-Blown Polyisocyanurate Foam System for Metal-Faced Continuous Sandwich Panels" *Journal of Cellular Plastics* 2002, Vol.38, pp.385-401
- [54] Gilbert D.R. "Index Versus Flammability in Urethane Modified Isocyanurate Foam Systems" *Journal of Cellular Plastics* 1986, Vol.22, pp.69-79
- [55] Gibson L.J., Ashby M.F. "Cellular Solids Structure and Properties" second edition, Oxford: Pergamon Press; 1997
- [56] Andersons J., Kirpluks M., Stiebra L., Cabulis U. "Anisotropy of the stiffness and Strength of Rigid Low-density Closed-cell Polyisocyanurate Foams" *Materials and Design* 2016, Vol.92, pp.836-845
- [57] De Gisi S.L., Neet T.E. "Predicting the Compressive Properties of Rigid Urethane Foam" *Journal of Applied Polymer Science* 1976, Vol.20, pp.2011-2029
- [58] Goods S.H., Neuschwanger C.L., Henderson C., Skala D.M. "Mechanical Properties of CRETE, a Polyurethane Foam" *Journal of Applied Polymer Science* 1998, Vol.68, pp.1045-1055
- [59] Hamilton A.R., Thomsen O.T., Madaleno L.A.O., Jensen L.R., Rauhe J.C.M., Pyrz R. "Evaluation of the anisotropic mechanical properties of reinforced polyurethane foams" *Composites Science and Technology* 2013, Vol.87, pp.210-217
- [60] Traeger R.K., Hermansen R.D. "Properties of Structural Foams" *Journal of Cellular Plastics* 1971, Vol.7 (N°4), pp.189-194
- [61] Goods S.H., Neuschwanger C.L., Henderson C., Skala D.M. "Mechanical Properties and Energy Absorption Characteristics of a Polyurethane Foam" Sandia National Laboratories Report # SAND97-8490, 1997
- [62] Gupta V.K., Khakhar D.V. "Formation of Integral Skin Polyurethane Foams" *Polymer Engineering and Science* 1999, Vol.39, pp.164-176
- [63] Harbron D.R., Page C.J., Scarrow R.K. "Methods of Minimising Density Gradients in Rigid Polyurethane Foams" *Journal of Cellular Plastics* 2001, Vol.37, pp.43-57

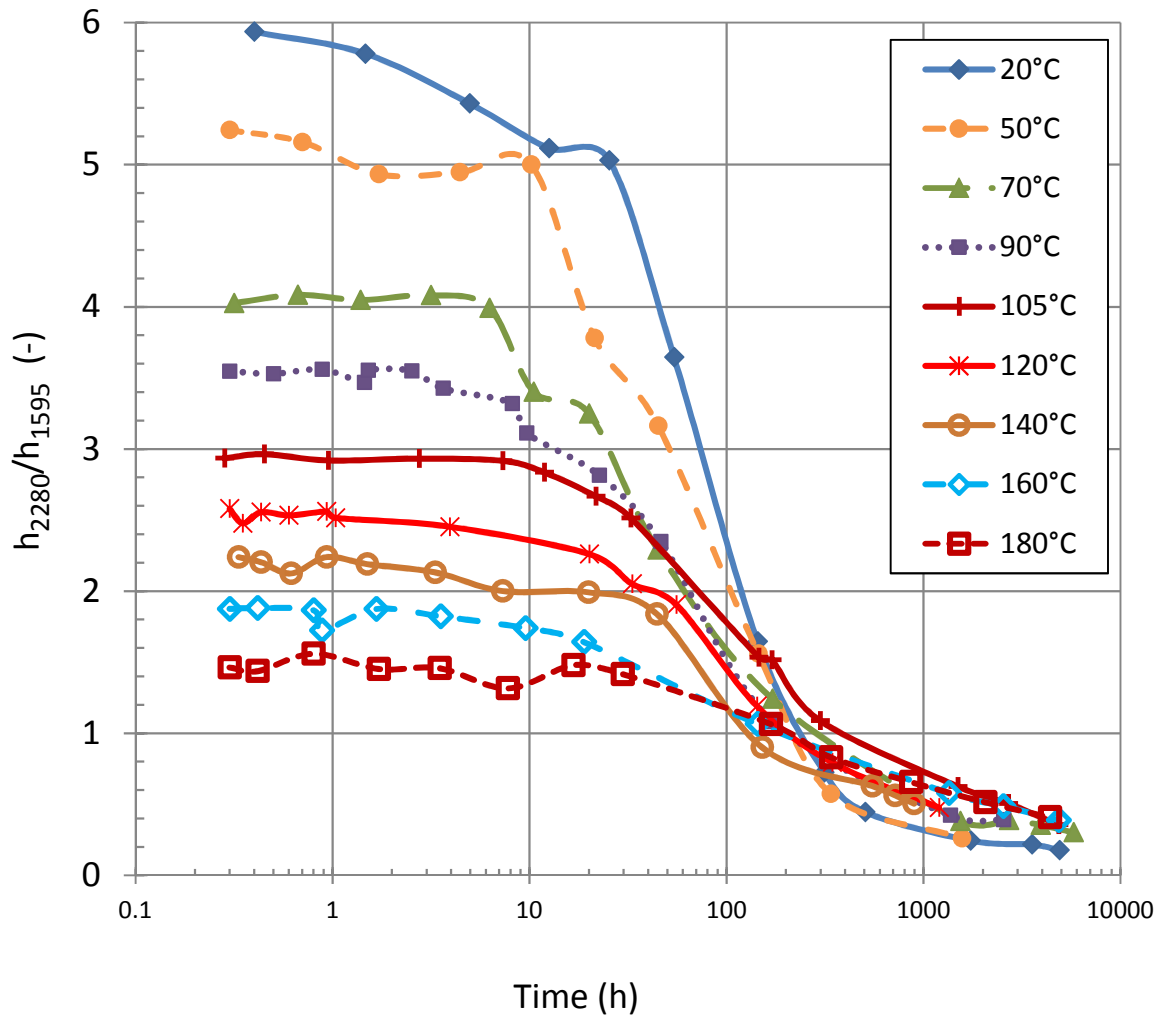
- [64] Modesti M., Adriani V., Simioni F. "Chemical and Physical Blowing Agents in Structural Polyurethane Foams: Simulation and Characterization" *Polymer Engineering and Science* 2000, Vol.40, pp.2046-2057
- [65] Jackovich D., O'Toole B., Hawkins M.C., Sapochak L. "Temperature and Mold Size Effects on Physical and Mechanical Properties of a Polyurethane Foam" *Journal of Cellular Plastics* 2005, Vol.41, pp.153-168
- [66] Peng S., Jackson P., Sendjarevic V., Frisch K.C., Prentice G.A., Fuchs A., "Process Monitoring and Kinetics of Rigid Poly(urethane-isocyanurate) Foams" *Journal of Applied Polymer Science* 2000, Vol.77 (N^o2), pp.374-380
- [67] Ashida K., Saiki K., Goto J., Sasaki K. "Polyisocyanurate Foams Modified by Thermally Stable Linkages" *ACS Symposium Series* 1997, Vol.669 "Polymeric Foams", pp.81-100
- [68] Delebecq E., Pascault J.-P., Boutevin B, Ganachaud F. "On the Versatility of Urethane/Urea Bonds: Reversibility, Blocked Isocyanate, and Non-Isocyanate Polyurethane" *Chemical Reviews* 2012, Vol.113, pp.80-118
- [69] Simon J., Barla F., Kelemen-Haller A., Farkas F., Kraxner M., "Thermal Stability of Polyurethanes" *Chromatographia* 1988, Vol.25, pp.99-106
- [70] Ridha M., Shim V.P.W. "Microstructure and Tensile Mechanical Properties of Anisotropic Rigid Polyurethane Foam" *Experimental Mechanics* 2008, Vol.48, pp.763-776
- [71] Dawson J.R., Shortall J.B. "The Microstructure of Rigid Polyurethane Foams" *Journal of Materials Science* 1982, Vol.17, pp.220-224
- [72] Hatchett D.W., Kinyanjui J.M. "FTIR Analysis of Chemical Gradients in Thermally Processed Molded Polyurethane Foam" *Journal of Cellular Plastics* 2007, Vol.43, pp.183-196
- [73] Smits G.F. "Effect of Cellsize Reduction on Polyurethane Foam Physical Properties" *Journal of Thermal Insulation and Building Envelopes* 1994, Vol.17, pp.309-329
- [74] Huber A.T., Gibson L.J. "Anisotropy of Foams" *Journal of Materials Science* 1988, Vol.23, pp.3031-3040
- [75] Hawkins M.C., O'Toole B., Jackovich D. "Cell Morphology and Mechanical Properties of Rigid Polyurethane Foam" *Journal of Cellular Plastics* 2005, Vol.41, pp.267-285

Supplementary Information

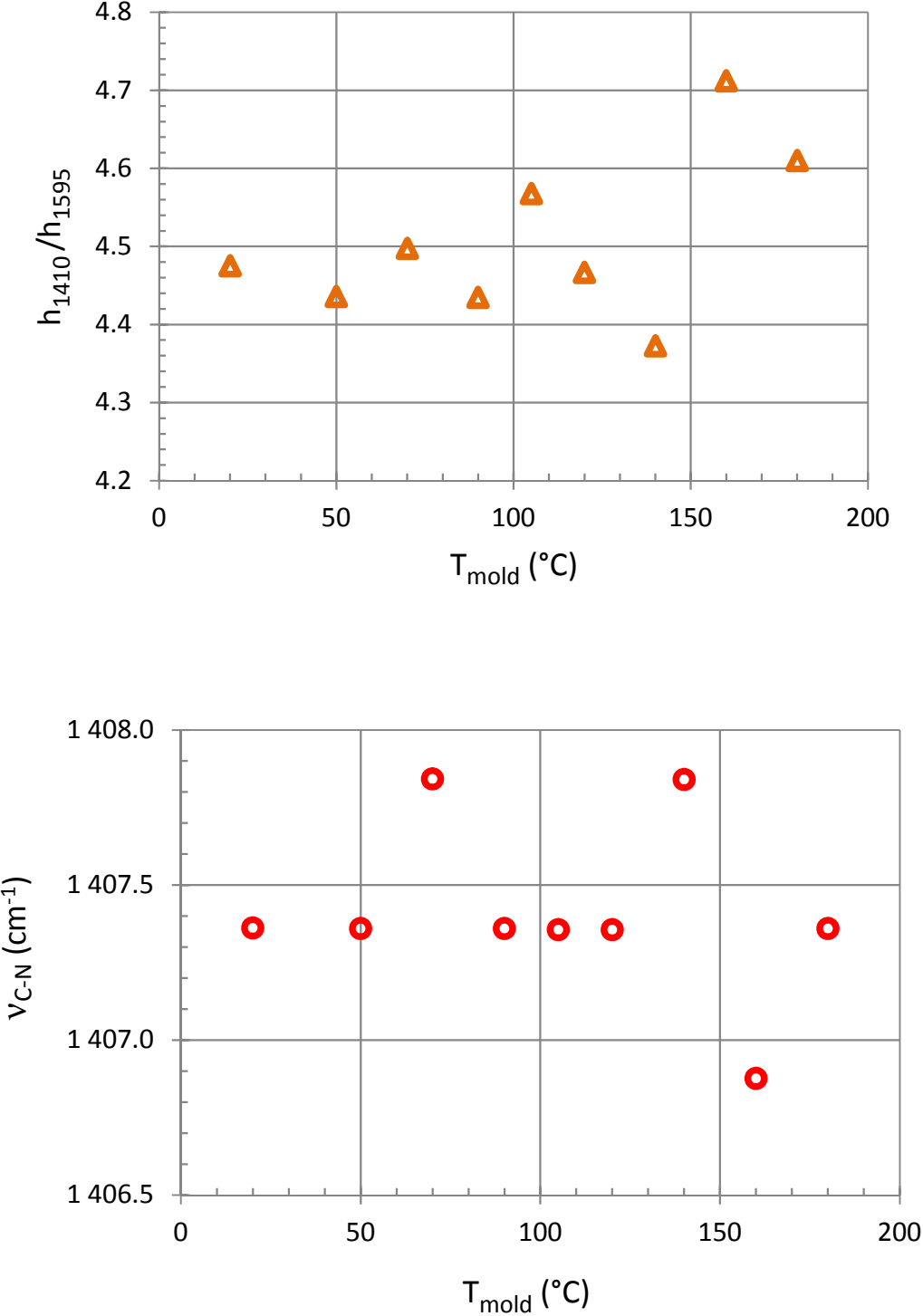
S11: Custom fabricated aluminum mold with a square base measuring 25 cm x 25 cm and a height of 15 cm. The bottom face of the mold was covered with a gas-tight facing typically used in foam insulation boards up to $T_{\text{mold}}=120^{\circ}\text{C}$ that was replaced by an aluminum foil for $T_{\text{mold}}>120^{\circ}\text{C}$. The lateral faces of the mold were covered with printer paper using double-sided mounting tape in order to protect the vertical wall of the mold and facilitate the removing of the foam bun after 15 min of cure. As can be seen from the photograph, the mold was open at the top to allow the foam to rise and expand freely.



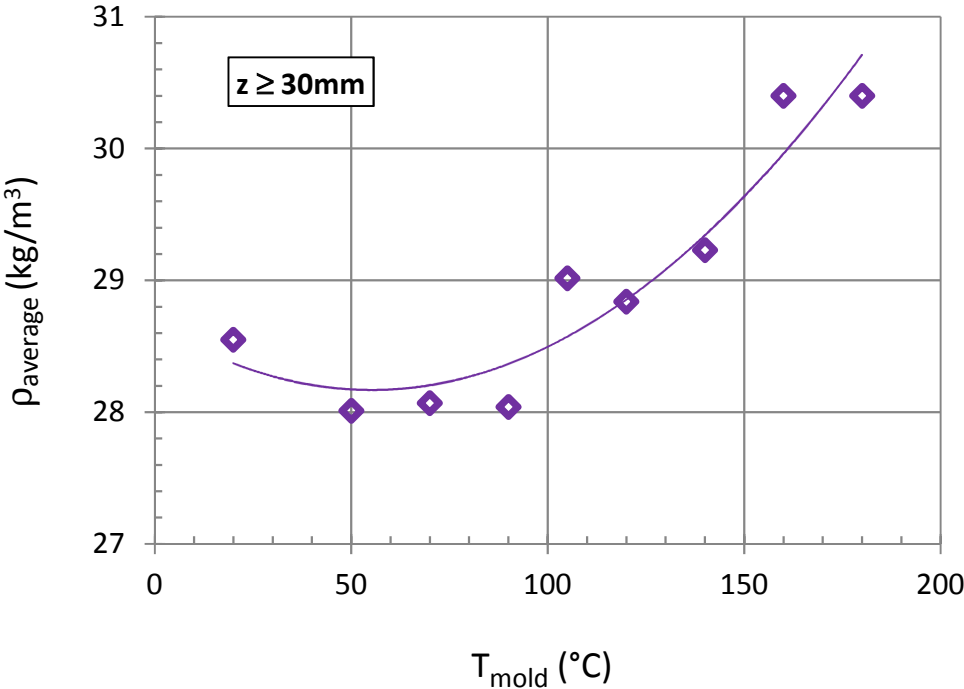
S12: Effect of time on the h_{2280}/h_{1595} (isocyanate/phenyl) peak height ratio for the surface (under the facing). Note that only part of the data was plotted so as not to overload the graphic. The lines are only guides for the eyes.



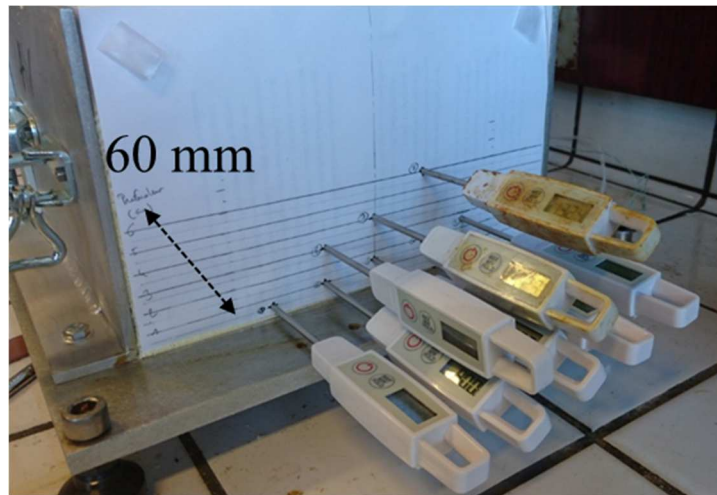
S13: Evolution of isocyanurate/phenyl ratio (h_{1410}/h_{1595}) and/or isocyanurate peak maximum (ν_{C-N}) of the foam core ($55 \text{ mm} \leq z \leq 60 \text{ mm}$) as a function of the mold temperature ($t \sim 4500 \text{ h}$)



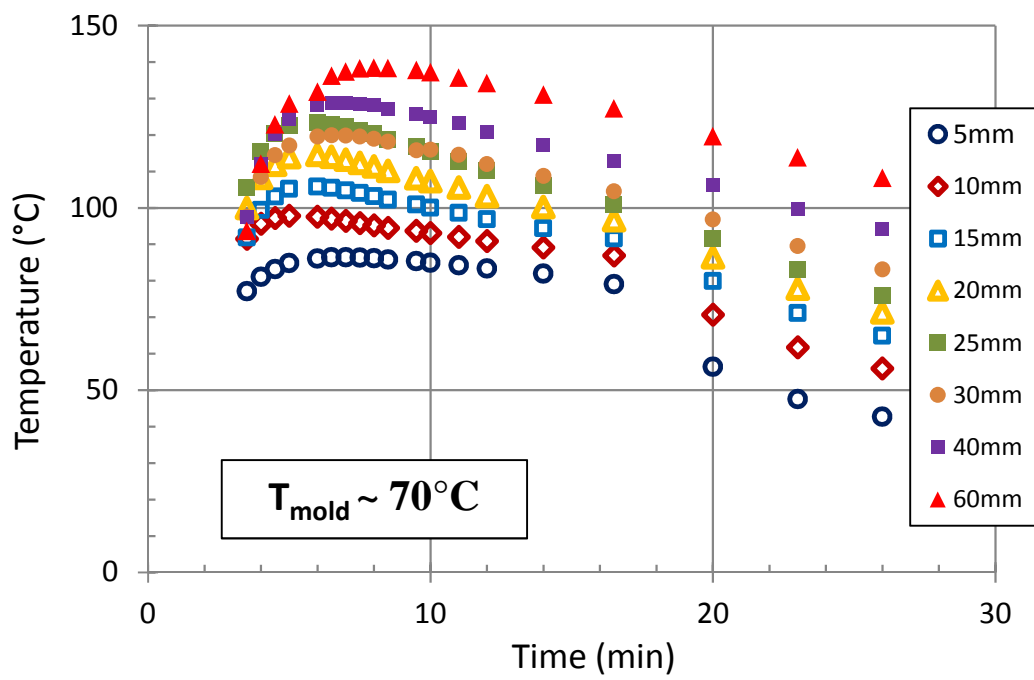
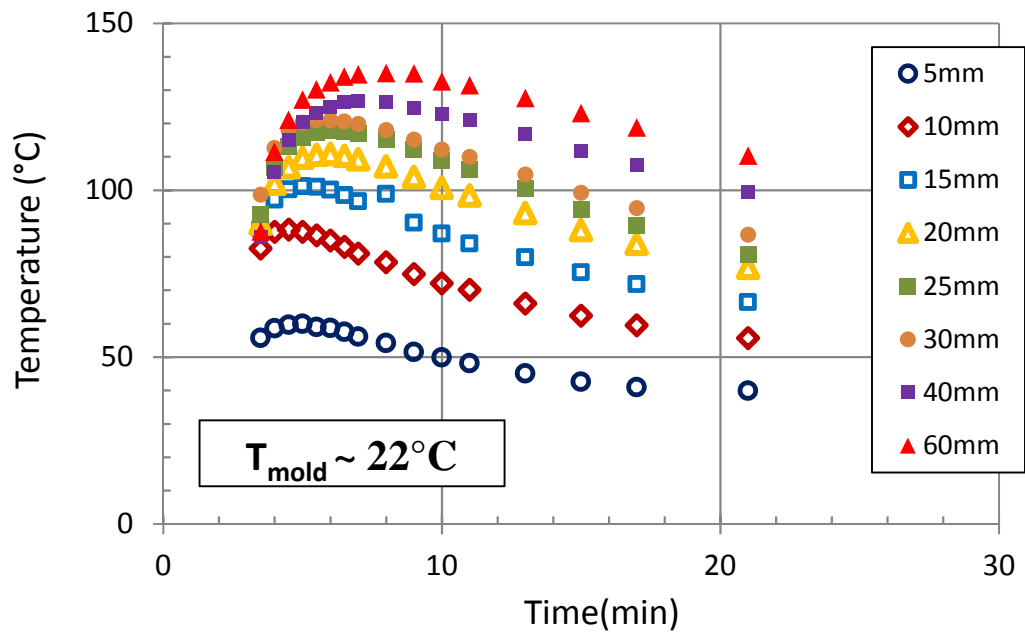
S14: Evolution of the average density of the foam core ($30 \text{ mm} \leq z \leq 60 \text{ mm}$) as a function of the mold temperature ($t \sim 4500 \text{ h}$). The line is only a guide for the eyes.

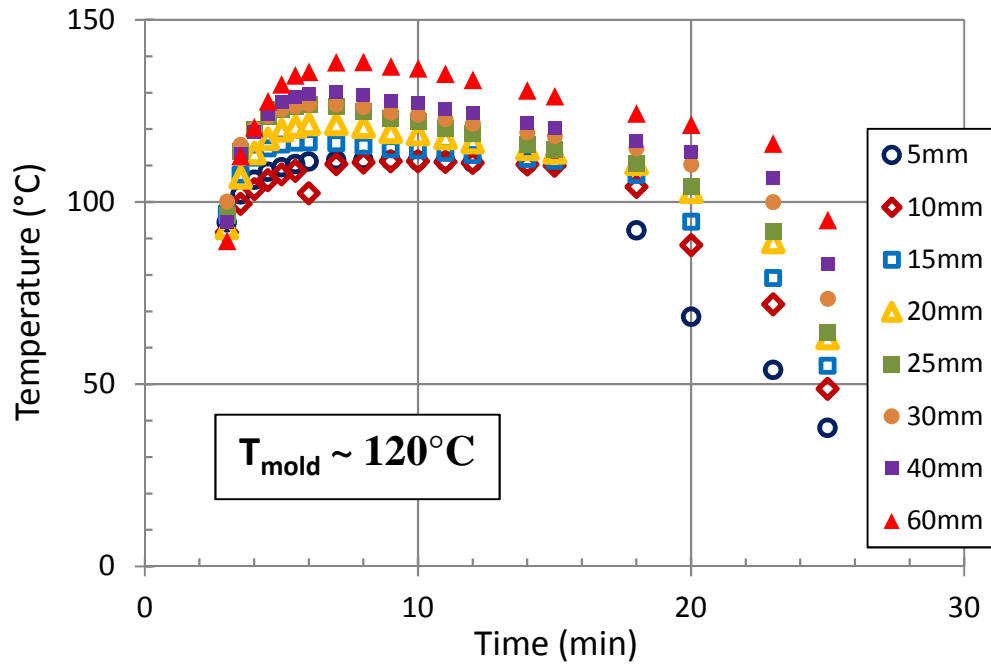


S15: Estimation of temperature profile during manufacturing between the core and the surface of the foam.



Additional experiments were carried out to follow the evolution of internal temperature as a function of time and for different z -depths (as a reminder, $z=0$ at the level of the facing). For that purpose, 8 thermometers were quickly introduced into the side of the foam (the lateral penetration depth was set to about 60 mm) after removing one of the lateral faces (as soon as the foam expansion is achieved, which takes about 2 min). It is worth noting that the foam block was removed from the mold at $t \sim 16$ min in order to follow the same experimental procedure, sometimes inducing a sudden decrease in the curves obtained near the surface. The $T=f(z,t)$ curves are shown below for 3 different mold temperatures ($T_{\text{mold}} \sim 22^\circ\text{C}$, $T_{\text{mold}} \sim 70^\circ\text{C}$ and $T_{\text{mold}} \sim 120^\circ\text{C}$).



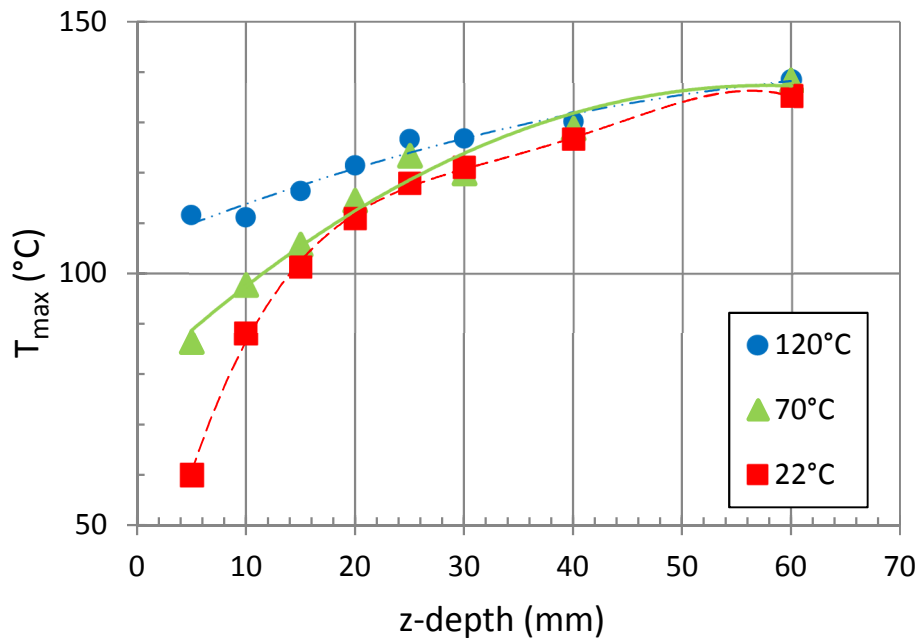


A few interesting comments can be made:

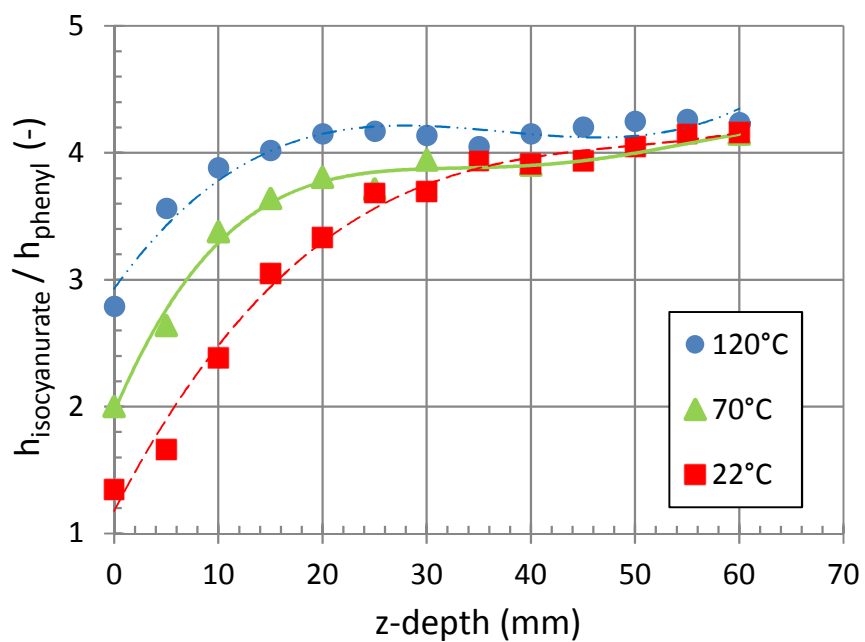
(i) Obviously, the maximum temperature (T_{max}) reached during foaming was found to increase with the z-depth (for each T_{mold}).

(ii) In addition, the higher the T_{mold} , the higher the value of T_{max} for the foam close to the surface ($z=5\text{mm}$) while the foam layer in the core ($z=60\text{mm}$) did not seem to be affected by T_{mold} . This is clearly illustrated in the graph showing the evolution of T_{max} as a function of z-depth (see below).

(iii) The change in cooling rate (dT/dt) is clearly visible at $t \sim 16$ min for the $T_{\text{mold}} \sim 120^{\circ}\text{C}$ and $z=5$ mm while the value of dT/dt does not seem to be affected in the core of the foam ($z=60$ mm).



These latter samples corresponding to T_{mold} of 22°C, 70°C and 120°C were also analyzed by FTIR-ATR from the surface to a depth of 60 mm. The evolution of isocyanurate/phenyl ratio of PIR foams is plotted as a function of z-depth in the next Figure. As expected, the h_{1410}/h_{1595} peak height ratio increases from the surface toward the inside of the foam and all $h_{1410}/h_{1595}=f(z)$ curves converge to the average value slightly greater than 4.



More interestingly, the evolution of isocyanurate/phenyl ratio is presented below as a function of T_{max} (The dashed line corresponds to the best-fit line through all the data points with a second-order polynomial equation; $R^2 \sim 0.91$). Clearly, the various data points seem to follow the same master curve which tends to demonstrate that the isocyanurate content is directly related to the maximum temperature (T_{max}) reached during foaming, regardless of the z-depth and/or T_{mold} . Note that the minor discrepancies could be related to different time (Δt) spent around T_{max} for each data point.

